

1 **Exploring the impacts of unprecedented climate extremes on forest ecosystems: hypotheses**
2 **to guide modeling and experimental studies**

3
4 Jennifer A. Holm^{1,*}, David M. Medvigy², Benjamin Smith^{3,4}, Jeffrey S. Dukes⁵, Claus Beier⁶,
5 Mikhail Mishurov³, Xiangtao Xu⁷, Jeremy W. Lichstein⁸, Craig D. Allen⁹, Klaus S. Larsen⁶, Yiqi
6 Luo¹⁰, Cari Ficken¹¹, William T. Pockman¹², William R.L. Anderegg¹³, and Anja Rammig¹⁴

7
8 ¹ Lawrence Berkeley National Laboratory, Berkeley, California, USA

9 ² University of Notre Dame, Notre Dame, Indiana, USA

10 ³ Dept of Physical Geography and Ecosystem Science, Lund University, Lund, Sweden

11 ⁴ Hawkesbury Institute for the Environment, Western Sydney University, Penrith, NSW 2751,
12 Australia

13 ⁵ Department of Forestry and Natural Resources and Biological Sciences, Purdue University,
14 West Lafayette, Indiana, USA

15 ⁶ Department of Geosciences and Natural Resource Management, University of Copenhagen,
16 Frederiksberg, Denmark

17 ⁷ Department of Ecology and Evolutionary Biology, Cornell University, Ithaca, New York, USA

18 ⁸ Department of Biology, University of Florida, Gainesville, Florida, USA

19 ⁹ U.S. Geological Survey, Fort Collins Science Center, New Mexico Landscapes Field Station,
20 Los Alamos, New Mexico, USA

21 ¹⁰ Center for Ecosystem Science and Society, Department of Biological Sciences, Northern
22 Arizona University, Flagstaff, Arizona, USA

23 ¹¹ Department of Biology, University of Waterloo, Waterloo, Ontario, Canada

24 ¹² Department of Biology, University of New Mexico, Albuquerque, New Mexico, USA

25 ¹³ School of Biological Sciences, University of Utah, Salt Lake City, Utah, USA

26 ¹⁴ Technical University of Munich, TUM School of Life Sciences Weihenstephan, Freising,
27 Germany

28

29 * *Correspondence to:* Jennifer Holm; 510-495-8083; jaholm@lbl.gov

30

31 **Keywords:** demographic modeling; mortality; drought; recovery; carbon cycle; nonstructural
32 carbohydrate storage; plant hydraulics; dynamic vegetation

33

34 **Abstract**

35

36 Climatic extreme events are expected to occur more frequently in the future, increasing the
37 likelihood of unprecedented climate extremes (UCEs), or record-breaking events. UCEs, such as
38 extreme heatwaves and droughts, substantially affect ecosystem stability and carbon cycling by
39 increasing plant mortality and delaying ecosystem recovery. Quantitative knowledge of such
40 effects is limited due to the paucity of experiments focusing on extreme climatic events beyond
41 the range of historical experience. Here, we present a road map of how dynamic vegetation
42 demographic models (VDMs) can be used to investigate hypotheses surrounding ecosystem
43 responses to one type of UCE; unprecedented droughts. As a result of nonlinear ecosystem
44 responses to UCEs, that are qualitatively different from responses to milder extremes, we
45 consider both biomass loss and recovery rates over time, by reporting a time-integrated carbon
46 loss as a result of UCE, relative to the absence of drought. Additionally, we explore how
47 unprecedented droughts in combination with increasing atmospheric CO₂ and/or temperature
48 may affect ecosystem stability and carbon cycling. We explored these questions using
49 simulations of pre-drought and post-drought conditions at well-studied forest sites, using equally
50 well-tested models (ED2 and LPJ-GUESS). The severity and patterns in biomass losses differed
51 sustainably between models. For example, biomass loss could be sensitive to either drought
52 duration or drought intensity depending on the model approach. This is due to the models having
53 different, but also plausible representations of processes and interactions, highlighting the
54 complicated interactions and variability of UCE impacts still needed to be narrowed down in
55 models. Elevated atmospheric CO₂ concentrations (eCO₂) alone did not completely buffer the
56 ecosystems from carbon losses during UCEs in the majority of our simulations. Our findings
57 highlight contrasting differences in process formulations and uncertainties in models, most
58 notably related to availability in plant carbohydrate storage and the diversity of plant hydraulic
59 schemes, in projecting potential ecosystem responses to UCEs. We provide a summary of the
60 current state and role of many model processes that give way to different underlying hypotheses
61 of plant responses to UCEs, reflecting knowledge gaps, which in future studies could be tested
62 with targeted field experiments and an iterative modeling-experimental conceptual framework.

Deleted: two

Deleted: s

Deleted: (e.g.,

Deleted:)

Deleted: the

Deleted: ED2 and LPJ-GUESS

Deleted: Due to the two models having different but plausible representations of processes and interactions, they diverge in sensitivity of nonlinear biomass loss due to drought duration or intensity, and differ between each site.

Deleted: B

Deleted: are most

Deleted: in ED2, but to

Deleted: in LPJ-GUESS

Formatted: Not Highlight

Formatted: Not Highlight

Formatted: Not Highlight

Deleted: should

78 **1 Introduction**

79 The increase in extreme climate and weather events, such as prolonged heatwaves and
80 droughts as seen over the last three decades, are expected to continue to increase in frequency
81 and magnitude, leading to progressively longer and warmer droughts on land (IPCC 2012, 2021).
82 Droughts are affecting all areas of the globe, more than any other natural disturbance, and recent
83 droughts have broken long-standing records (Ciais et al., 2005; Phillips et al., 2009; Williams et
84 al., 2012; Matusick et al., 2013; Griffin and Anchukaitis, 2014; Asner et al., 2016; Feldpausch et
85 al., 2016; Seneviratne et al., 2021). Such ‘unprecedented climate extremes’ (UCEs; “record-
86 breaking events”, IPCC (2012)) that are larger in extent and longer-lasting than historical norms
87 can have dramatic consequences for terrestrial ecosystem processes, including carbon uptake and
88 storage and other ecosystem services (Reichstein et al., 2013; Settele, 2014; Allen et al., 2015;
89 Brando et al., 2019; Kannenberg et al., 2020). Thus, to better anticipate the implications of
90 climatic changes for the terrestrial carbon sink and other ecosystem services, we need to better
91 understand how ecosystems respond to extreme droughts and other UCEs.

92 To learn how ecosystems respond to rarely experienced or unprecedented conditions,
93 ecologists can experimentally manipulate environmental conditions (Rustad, 2008; Beier et al.,
94 2012; Meir et al., 2015; Aguirre et al., 2021). However, the majority of such experiments apply
95 moderate treatments based on a historical sense, which are mostly weaker in intensity and/or
96 shorter in duration than potential future UCEs (Beier et al., 2012; Kayler et al., 2015; but see Luo
97 et al., 2017), and single experiments have low power to detect effects of stressors on ecosystem
98 responses (Yang et al., 2022). Additionally, most experiments examine low-stature ecosystems,
99 such as grassland, shrubland or tundra, due to lower requirements for infrastructure and financial
100 investment compared to mature forests. However, forests may respond qualitatively differently
101 to UCEs than other ecosystems, in part due to mortality of large trees and strong nonlinear
102 ecosystem responses, with long-lasting consequences for ecosystem-climate feedbacks (Williams
103 et al., 2014; Meir et al., 2015). Ecosystem responses to naturally occurring extreme droughts and
104 heatwaves have been documented (Ciais et al., 2005; Breshears et al., 2009; Feldpausch et al.,
105 2016; Matusick et al., 2016; Ruthrof et al., 2018; Powers et al., 2020); however, these rapidly-
106 mobilized post-hoc studies often are unable to measure all critical variables and may lack
107 consistently collected data for comparison with pre-drought conditions, thus limiting their
108 inferential power and ability to improve quantitative models. The difficulties of performing

109 controlled real-world experiments of UCEs at broad spatial and temporal scales make process-
110 based modeling a valuable tool for studying potential ecosystem responses to extreme events.

111 Process-based models can be used to explore potential ecosystem impacts using projected
112 climate change over broad spatial and temporal scales (Gerten et al., 2008; Luo et al., 2008;
113 Zscheischler et al., 2014; Sippel et al., 2016), as seen in a few modeling studies that have
114 synthesized and improved our process-level understanding of UCE effects (McDowell et al.,
115 2013; Dietze and Matthes, 2014). However, due to the overly simplified representation of
116 ecological processes in most land surface models (LSMs) – the terrestrial components of Earth
117 System Models (ESMs) used for climate projections – it is doubtful whether most of these
118 models adequately capture ecosystem feedbacks and other responses to UCEs (Fisher and
119 Koven, 2020). For example, only a few ESMs in recent coupled model intercomparison projects
120 (CMIP6) (Arora et al., 2020; IPCC 2021) include vegetation demographics (Döscher et al.,
121 2022), and most rely on prescribed, static maps of plant functional types (PFTs) (Ahlström et al.,
122 2012). Other LSMs simulate PFT shifts (i.e., dynamic global vegetation models, DGVMs; Sitch
123 et al., (2008)) based on bioclimatic limits, instead of emerging from the physiology- and
124 competition-based demographic rates that determine resource competition and plant distributions
125 in real ecosystems (Fisher et al., 2018). While a new generation of LSMs with more explicit
126 ecological dynamics and structured demography is emerging (Holm et al., 2020; Koven et al.,
127 2020; Döscher et al., 2022), most current ESMs are limited in ecological detail and realism (e.g.,
128 ecosystem structure, demography, and disturbances). Failing to mechanistically represent
129 mortality, recruitment, and disturbance – each of which influences biomass turnover and carbon
130 (C) allocation (Friend et al., 2014) – limits the ability of these models to realistically forecast
131 ecosystem responses to anomalous environmental conditions like UCEs (Fisher et al., 2018).

132 Evaluating and improving the representation of physiological and ecological processes in
133 ecosystem models is critical for reducing model uncertainties when projecting the effects of
134 UCEs on long-term ecosystem dynamics and functioning. Vegetation demography, plant
135 hydraulics, enhanced representations of plant trait variation, explicit treatments of resource
136 competition (e.g., height-structured competition for light), and representing major disturbances
137 (e.g., extreme drought) have all been identified as critical areas for advancing current models
138 (Scheiter et al., 2013; Fisher et al., 2015; Weng et al., 2015; Choat et al., 2018; Fisher et al.,
139 2018; Blyth et al., 2021) and are necessary advances for realistically representing the ecosystem

Deleted: and IPCC climate assessments

Deleted: Ciais et al., 2013;

Deleted: Although

143 impacts of UCEs. In this perspectives focused paper we look at the differences in these
144 processes, and how they contribute to uncertainty across multiple temporal phases surrounding
145 an extreme event: predicting an ecosystem's pre-disturbance resistance, which influences the
146 degree of impact and recovery from UCEs. Table 1 describes a summary of model mechanisms
147 that affect pre-drought resistance and post-drought recovery and we suggest are critical areas
148 further research (ca. Frank et al., 2015).

149 In order to inform our discussion, we explore the potential responses of forest ecosystems
150 to UCEs using two state-of-the-art process-based demographic models (vegetation demographic
151 models, VDMs; Fisher et al., (2018)), a unique model exploration-discussion approach to help
152 highlight new paths forward for model advancement. We first present conceptual frameworks
153 and hypotheses on potential ecosystem responses to UCEs based on current knowledge. We then
154 present VDM simulations for a range of hypothetical UCE scenarios to illustrate current state-of-
155 the-art model representations of eco-physiological mechanisms expected to drive responses to
156 UCEs, [using droughts as an example](#). While a variety of UCE-linked biophysical tree
157 disturbance processes (e.g., fire, wind, insect outbreaks) can drive nonlinear ecosystem
158 responses, we focus specifically on extreme droughts, which have important impacts on many
159 ecosystems around the world (e.g. Frank et al., 2015, IPCC 2021). By studying modeled
160 responses to UCEs, we explore the limits to our current understanding of ecosystem responses to
161 extreme droughts and their corresponding thresholds and tipping points. As anthropogenic
162 forcing has increased the frequency, duration, and intensity of droughts throughout the world
163 (Chiang et al., 2021), we explore how eCO₂ and rising temperatures may affect drought-induced
164 C loss and recovery trajectories. [This study can help guide](#) how the scientific community can
165 iteratively address these questions through [future](#) experiments and modeling studies. We believe
166 the combination of using cutting-edge VDMs alongside an inspection of current gaps in
167 knowledge will help guide modeling and experimental advances in order to address novel forest
168 responses to climate extremes.

169

170 **1.1 Conceptual and Modeling Framework for Hypothesis Testing:**

171 We combine conceptual frameworks (Fig. 1) and ecosystem modeling to test two
172 hypotheses on potential responses of plant carbon stocks to UCEs. The first hypothesis is:

Deleted: , and

174 **Hypothesis (H1). Terrestrial ecosystem responses to UCEs will differ qualitatively from**
175 **ecosystem responses to milder extremes because responses are nonlinear and highly variable.**
176 **Nonlinearities can arise from multiple mechanisms – including shifts in plant hydraulics, C**
177 **allocation, phenology, and stand demography – and can vary depending on the pre-drought**
178 **state of the ecosystem.**

179 We present three conceptual relationships that describe terrestrial ecosystem responses to
180 varying degrees of extreme events (Fig. 1). We hypothesize that change in vegetation C stock is
181 related to drought intensity and/or drought duration, such that biomass loss increases nonlinearly
182 with increased drought intensity (i.e., reduction in precipitation) represented by a threshold-based
183 relationship (Fig. 1a, H1a), increased drought duration (i.e., prolonged drought with the same
184 intensity) by shifting responses typically seen in milder extremes downwards via increasing
185 slopes (Fig. 1a, H1b), or the combination of both intensity and duration (Fig. 1a, H1c). These
186 hypotheses are supported by observations from the Amazon Basin and Borneo (Phillips et al.,
187 2010) where tree mortality rates increased nonlinearly with drought intensity. Similarly, plant
188 hydraulic theories predict nonlinear damage to the plant-water transport systems, and thus
189 mortality risk, as a function of drought stress (Sperry and Love, 2015). In particular, longer
190 droughts are more likely to lead to lower soil water potentials, leading to a nonlinear xylem
191 damage function even if stomata effectively limit water loss (Sperry et al., 2016).

192 **Hypothesis (H2): The effects of increasing atmospheric CO₂ concentration (eCO₂) will**
193 **alleviate impacts of extreme drought stress through an increase in vegetation productivity and**
194 **water-use efficiency, but only up to a threshold of drought severity, while increased**
195 **temperature (and related water stress) will exacerbate tree mortality.**

196 This second hypothesis is based on growing evidence that effects of eCO₂ and climate
197 warming may interact with effects of drought intensity on ecosystems. The CO₂ fertilization
198 effect enhances vegetation productivity (e.g., net primary production, NPP) (Ainsworth and
199 Long, 2005; Norby et al., 2005; Wang et al., 2012), but this fertilization effect is generally
200 reduced by drought (Hovenden et al., 2014; Reich et al., 2014; Gray et al., 2016). Drought events
201 often coincide with increased temperature, which intensifies the impact of drought on
202 ecosystems (Allen et al., 2015; Liu et al., 2017), resulting in nonlinear responses in mortality
203 rates (Adams et al., 2009; Adams et al., 2017a). The evaluation of C cycling in VDMs with

Deleted: four

Deleted: C

Deleted: in a near-linear relationship (Fig. 1a, H0, null hypothesis), which has some observational support from annual and perennial grassland ecosystems, shrublands and savannas across the globe (Bai et al., 2008; Muldavin et al., 2008; Ruppert et al., 2015). We recognize that most ecological systems are nonlinear, thus alternatives to the null hypothesis are

Deleted: the near-linear relationship

214 doubling of CO₂ (only “beta effect”) showed a large carbon sink in a tropical forest (Holm et al.,
215 2020), but the inclusion of climate interactions in VDMs needs to be further explored.

216 Here, we relate ecosystem responses to UCEs by calculating a “~~severity-drought index~~”
217 (Fig. 1b and see Methods), which integrates C loss from the beginning of the drought until the
218 time when C stocks have recovered to 50% of the pre-drought level. In response to drought,
219 warming, and eCO₂, divergent potential C responses (gains and losses; Fig. 1c) can be expected
220 (Keenan et al., 2013; Zhu et al., 2016; Adams et al., 2017a). For example, a grassland
221 macrocosm experiment found that eCO₂ completely compensated for the negative impact of
222 extreme drought on net carbon uptake due to increased root growth and plant nitrogen uptake,
223 and led to enhanced post-drought recovery (Roy et al., 2016). However, a 16-year grassland
224 FACE and the SoyFACE experiments showed that CO₂ fertilization effects were reduced or
225 eliminated under hotter/drier conditions (Gray et al., 2016; Obermeier et al., 2016). Reich et al.,
226 (2014) also found that CO₂ fertilization effects were reduced in a perennial grassland by water
227 and nitrogen limitation.

228 A corollary to our H2 is that conditions that favor productivity (e.g., longer growing
229 seasons and/or CO₂ fertilization) will enhance vegetation growth leading to “structural
230 overshoot” (SO; Fig. 1d; adapted from and supported by Jump et al., 2017), and can amplify the
231 effects of UCEs. Enhanced vegetation growth coupled with environmental variability can lead to
232 exceptionally high plant-water-demand during extreme drought and water stress, resulting in a
233 “mortality overshoot” (MO; Fig 1d). We conceptualize how oscillations between SO and
234 associated MO could be amplified by increasing climatic variability and UCEs (Fig. 1d).

235 ~~Additionally, more climatic variability from~~ unprecedented eCO₂ levels and ~~warming~~ will
236 ~~contribute to unknowns in how~~ ecosystems ~~are affected~~ in the future (i.e., the widening, ~~and~~
237 ~~downward shape~~ of the shaded areas compared to historical, Fig. 1d). We expect, however that a
238 rapidly changing climate, combined with effects of UCEs as a result of more frequent extreme
239 drought/heat events and drought stress, can exacerbate and amplify SOs and MOs (Jump et al.,
240 2017), leading to increasing C loss, even though various buffering mechanisms exist (cf. (Lloret
241 et al., 2012; Allen et al., 2015)). Relative to our conceptual (Fig. 1d), we note that most
242 experimental, observational and modeling studies (Ciais et al., 2005; da Costa et al., 2010;
243 Phillips et al., 2010; Meir et al., 2015) take into account only low to moderate drought intensities

Deleted: the

Deleted: integrated carbon (C) loss

Deleted: Confidence is low as to how historically

Deleted: temperatures

Deleted: affect

249 (such as 50% rain excluded) or single events, or combine drought with moderate effects of
250 temperature change. Where there has been 100% rain exclusion, it was on very small plots of 1.5
251 m² (Meir et al., 2015). As represented by the increasing amplitude of oscillations in Fig. 1d, the
252 interactions between increased temperatures, UCE events, and vegetation feedbacks make
253 ecosystem states become inherently unpredictable, particularly over longer time-scales.

254

255 **2 Vegetation Demography Model (VDM) Approaches**

256 We argue that VDMs are well suited to address climate change impacts due to the
257 inclusion of detailed process representation of dynamic plant growth, recruitment, and mortality,
258 resulting in changes in abundance of different PFTs, as well as vertically stratified tree size- and
259 age-class structured ecosystem demography. Community dynamics and age-/size-structure are
260 emergent properties from competition for light, space, water, and nutrients, which dynamically
261 and explicitly scale up from the tree, to stand, to ecosystem level. Within this characterization,
262 VDMs also differ between each other and are set up in different configuration, allowing for
263 various testing capabilities. For full names of each model listed below and references, see Table
264 S1. For example, VDMs can aggregate and track the community level disturbance into either
265 patch-tiling sampling (e.g., ED2, FATES, LM3-PPA, ORCHIDEE, JSBACH4.0) or statistical
266 approximations (e.g., LPJ-GUESS, SEIB-DGVM, and CABLE-POP). VDMs could also vary in
267 representing light competition within either multiple canopy layers (e.g., ED2, FATES, LM3-
268 PPA, LPJ-GUESS, SEIB-DGVM) or in a single canopy (e.g., JSBACH4.0, ORCHIDEE,
269 CABLE-POP).

270 Powell et al. (2013) compared multiple VDMs and LSMs to interpret ecosystem
271 responses to long-term droughts in the Amazon and are informative when conducting model-data
272 comparisons, but studies of the cascade of ecosystem responses and mortality to UCEs are
273 lacking. In a cutting-edge area of development, new mechanistic implementation of plant
274 competition for water and plant hydraulics in VDMs (i.e., hydrodynamics) are improving our
275 understanding of plant-water relations and stresses within plants, such as with TFSv.1-Hydro
276 (Christoffersen et al., 2016), ED2-hydro (Xu et al., 2016), and FATES-HYDRO (Ma et al., 2021;
277 Fang et al., 2022). Compared to more simplistic representation of plant acquiring soil moisture
278 not connected to plant physiology (e.g., LPJ-GUESS, LM3-PPA, CABLE-POP, SEIB-DGVM).

279 For hydrodynamic representations in ‘big-leaf’ LSMs such as CLM5, JULES, and Noah-MP-
280 PHS see Kennedy et al., (2019), Eller et al., (2020), and Li et al., (2021) respectively.

281 The discussion section provides a deeper investigation of model response to UCEs related
282 to droughts. An exhaustive review of all VDMs, and all plant processes is too large to be done
283 here. Existing review papers of different VDM development, processes, and uncertainties can be
284 found here: Fisher et al., (2018); Bonan (2019); Trugman et al., (2019); Hanbury-Brown et al.
285 (2022); Bugmann and Seidl (2022); and specifically related to plant hydraulics see: Mencuccini
286 et al., (2019); Anderegg and Venturas (2020). We use LPJ-GUESS and ED2 as example VDMs
287 in an initial guide framework to explore hypotheses around vegetation mortality and severity
288 index from UCEs and climate change impacts, and highlight limiting model processes. Since
289 field data needed to evaluate UCE responses are, by definition, unavailable, we do not perform
290 model-data comparisons. Rather, we use the model results and conceptual framework as a road
291 map to explore our hypotheses and illustrate their implications for ecosystem responses under
292 UCEs, not historical drought events.

293

294 **2.1 LPJ-GUESS and ED2 Model Descriptions**

295 We explored our hypotheses at forested ecosystems in Australia and Central America
296 using two VDMs: the Lund-Potsdam-Jena General Ecosystem Simulator (LPJ-GUESS) (Smith et
297 al., 2001; Smith et al., 2014) and the Ecosystem Demography model 2 (ED2) (Medvigy et al.,
298 2009; Medvigy and Moorcroft, 2012). Both LPJ-GUESS and ED2 resolve vegetation into tree
299 cohorts characterized by their PFT, in addition to age-class in LPJ-GUESS; and size, and stem
300 number density in ED2. Both models are driven by external environmental drivers (e.g.,
301 temperature, precipitation, solar radiation, atmospheric CO₂ concentration, nitrogen deposition),
302 and soil properties (soil texture, depth, etc.), and also depend on dynamic ecosystem state, which
303 includes light attenuation, soil moisture, and soil nutrient availability. Establishment and growth
304 of PFTs, and their carbon-, nitrogen- and water-cycles, are simulated across multiple patches per
305 grid cell to account for landscape heterogeneity. Both models characterize PFTs by physiological
306 and bioclimatic parameters, which vary between the models (Smith et al., 2001; Smith et al.,
307 2014; Medvigy et al., 2009; Medvigy and Moorcroft, 2012).

308 The LPJ-GUESS includes three woody PFTs: evergreen, intermediate evergreen, and
309 deciduous PFTs. Mortality in LPJ-GUESS is governed by a ‘growth-efficiency’-based function

Deleted: integrated carbon loss

311 (kg C m⁻² leaf yr⁻¹), which captures effects of water deficit, shading, heat stress, and tree size on
312 plant productivity relative to its resource-uptake capacity (leaf area), with a threshold below
313 which stress-related mortality risk increases markedly, in addition to background senescence and
314 exogenous disturbances. Stress mortality can be reduced by plants using labile carbon storage,
315 modeled implicitly using a ‘C debt’ approach, which buffers low productivity, enhancing
316 resilience to milder extremes (more details are given in section 4.1.4). Total mortality can thus be
317 impacted by variation in environmental conditions such as water limitation, low light conditions,
318 and nutrient constraints, as well as current stand structure (Smith et al., 2001; Hickler et al.,
319 2004).

320 The ED2 version used here (Xu et al., 2016) includes four woody PFTs: evergreen,
321 intermediate evergreen, deciduous, brevi-deciduous, and deciduous stem-succulent. This ED2
322 version includes coupled photosynthesis, plant hydraulics, and soil hydraulic modules (Xu et al.,
323 2016), which together determine plant water stress. The plant hydraulics module tracks water
324 flow along a soil–plant–atmosphere continuum, connecting leaf water potential, stem sap flow,
325 and transpiration, thus influencing controls on photosynthetic capacity, stomatal closure,
326 phenology, and mortality. Leaf water potential depends on time-varying environmental
327 conditions as well as time-invariant PFT traits. Leaf shedding is triggered when leaf water
328 potential falls below the turgor loss point (a PFT trait) for a sufficient amount of time. Leaf
329 flushing occurs when stem water potential remains high (above half of the turgor loss point) for a
330 sufficient time (see Xu et al., 2016 for details). PFTs differ in their hydraulic traits, wood
331 density, specific leaf area, allometries, rooting depth, and other traits. Stress-based mortality in
332 the ED2 version used here includes two main physiological pathways in our current
333 understanding of drought mortality (McDowell et al., 2013): C starvation and hydraulic failure.
334 Mortality due to C starvation in ED2 results from a reduction of C storage, a proxy for non-
335 structural carbohydrate (NSC) storage, which integrates the balance of photosynthetic gain and
336 maintenance cost under different levels of light and moisture availability. Mortality due to
337 hydraulic failure in ED2 is based on the percentage loss of stem conductivity. ED2 also includes
338 a density-independent senescence mortality rate based on wood density.

339 **2.2 Modeling guide**

340 To exemplify how VDMs can be tools to explore new hypotheses related to UCEs we
341 applied the models at two field sites, that were chosen due to being extensively studied and the
342 models used here have already been run at these sites and previously benchmarked against field
343 data (see Xu et al., 2016; Medlyn et al., 2016; Medvigy et al., 2019 for model-data validation).
344 The purpose of this paper was not to do a large multi-site comparison, but rather just select a few
345 for hypothesis testing. In addition, the two sites span a range of vegetation types and are in
346 warm, seasonally dry climates that are more likely to experience droughts in the future (Allen et
347 al., 2017). The first is a mature *Eucalyptus* (*E. tereticornis*) warm temperate-subtropical
348 transitional forest that is the site of the Eucalyptus Free Air CO₂ enrichment (EucFACE)
349 experiment in Western Sydney, Australia (Medlyn et al., 2016; Ellsworth et al., 2017; Jiang et
350 al., 2020). The second site is a seasonally dry tropical forest in the Parque Nacional Palo Verde
351 in Costa Rica (Powers et al., 2009). Site description details can be found in Supplement Text A.

352 We performed a 100-year “baseline” simulation for each model at each site driven by
353 constant, near ambient, atmospheric CO₂ (400 ppm) and recycled historical site-specific climate
354 data (1992-2011 for EucFACE and 1970-2012 for Palo Verde; Sheffield et al., (2006)), absent of
355 drought treatments. A detailed description of the meteorological data and initial conditions used
356 to drive the models is in the Supplementary Text A. The two models were previously tuned for
357 each site (Xu et al., 2016; Medlyn et al., 2016), and no additional site-level parameter tuning was
358 conducted here due to evaluating responses from hypothetical UCEs. To describe the ecosystem
359 impact of UCEs, we simulated 10 years of pre-drought conditions (continuing from the baseline
360 simulation), followed by drought treatments that differed in intensity and duration, followed by a
361 100-year post-drought recovery period. To explore the effects of drought intensity, we conducted
362 20 different artificial drought intensity simulations, in which precipitation during the whole year
363 is reduced by 5% to 100% of its original amount, in increments of 5%. To explore the effects of
364 drought duration, the 20 different drought intensities are maintained over 1, 2 and 4 years (Table
365 S2). We examined model responses of aboveground biomass, leaf area index (LAI), stem density
366 (number ha⁻¹), plant available soil water (mm), plant C storage (kg C m⁻²), change in stem
367 mortality rate (yr⁻¹), and PFT composition.

368 To explore how temperature, eCO₂ concentration, and UCE droughts influence forest C
369 dynamics individually and in combination, we implemented the following five experimental
370 scenarios, some realistic and others hypothetical, for each model (Table S2): increased

371 temperature only (+2K over ambient), eCO₂ only (600 ppm and 800 ppm), and both increased
 372 temperature and eCO₂ (+2K 600 ppm; +2K 800 ppm). Temperature and eCO₂ manipulations
 373 were applied as step increases over the baseline conditions, and are artificial scenarios, as
 374 opposed to model-generated climate projections.

375

376 2.3 Linking concepts, hypotheses, and model outcomes

377 To relate our simulation results to Fig. 1a, we compared the total biomass loss as a result
 378 of each drought treatment by calculating the percentage of biomass reduction at the end of the
 379 drought period relative to the baseline (no drought) simulation. To explicitly consider biomass
 380 recovery rates over time, we calculated “**severity-drought index**” (Eqs. 1-3), as a result of
 381 drought under current climate, which are determined based on the concepts in Fig. 1b. We
 382 defined “**severity-drought index**” as the time-integrated carbon in biomass that is lost due to
 383 drought relative to what the vegetation would have stored in the absence of drought. That is, it is
 384 the difference between biomass in the presence of drought (B_d) at time (t) and biomass in the
 385 baseline simulation (no drought; B_{base}), integrated over a defined recovery time period (in kg C
 386 m⁻² yr):

$$387 \quad \text{Severity-drought index} = \int_{t=t_1}^{t=t_2} (B_{base}(t) - B_d(t)) dt \quad (\text{Eq. 1})$$

388 To define the bounds of integration, in Eq. 1, t_1 is defined as the time when the maximum
 389 amount of plant C is lost as a result of the drought:

$$390 \quad B_{base}(t_1) - B_d(t_1) = \max_t [B_{base}(t) - B_d(t)] \quad (\text{Eq. 2})$$

391 Then, t_2 is defined implicitly as the time when 50% of the lost biomass has been recovered
 392 compared to the baseline:

$$393 \quad B_{base}(t_2) - B_d(t_2) = \frac{1}{2} (B_{base}(t_1) - B_d(t_1)) \quad (\text{Eq. 3})$$

394 Since all **severity-drought index** results are taken as the difference from a non-drought baseline
 395 biomass (B_{base}) and all droughts will result in a loss of C.

396 We also use **the severity-drought index as a starting point** to examine the role of drought,
 397 temperature and eCO₂ change for moderating or exacerbating the impacts of drought on forest C

Deleted: integrated-C-loss

Deleted: integrated-C-loss

$$\text{Integrated-C-loss} = \int_{t=t_1}^{t=t_2} (B_{base}(t) - B_d(t)) dt$$

Deleted:

Formatted: Centered

Deleted: integrated-C-loss

Deleted: integrated-C-loss

403 stocks; i.e., to evaluate the hypotheses illustrated in Fig. 1c. To assess these impacts of changing
 404 climates, we calculate a **severity-climate index** (Eq. 4). Defined as the difference between the
 405 **severity-drought index** due to drought alone (Eqs. 1-3) under present climate, and the **severity**
 406 **index** due to the combined effects of drought and climate change (i.e., five scenarios of
 407 temperature increase and eCO₂), **still integrated over time to account for recovery:**

$$\text{Severity-climate index} = \text{Severity-drought index}_{\text{drought}} - \text{Severity-drought index}_{\text{drought+CC}} \quad (\text{Eq. 4})$$

409 Because we expect drought to reduce vegetation C stocks, and thus **severity-climate**
 410 **index** to be negative, positive values of **severity-climate index** indicate that changes in climatic
 411 drivers **ameliorate** the C losses from drought (i.e., buffering effects). Negative values of **severity-**
 412 **climate index** indicate that the climate change scenario leads to either greater C losses or losses
 413 that persist for longer amounts of time (i.e., magnitude and/or duration) compared to a simulation
 414 with no climate change (i.e., “**control**” run).
 415
 416

417 3 Results

418 As a basis for the treatment results presented here, we compared the baseline simulations
 419 (prior to drought or climate change treatments) of the two VDMs **against** observations, **and found**,
 420 **strong model validation at both sites** (Table S3, Fig. S1, **Supplemental Text A**). These models are
 421 well documented and investigated VDMs, with many studies that have looked into parameter
 422 uncertainty (see Supplemental Text A for select references that explore model/parameter
 423 sensitivity).

424 **The** models displayed **varied** nonlinear responses to drought, **differing substantially** in
 425 their behavior and between sites. In general, ED2 shows sensitivity to drought duration
 426 (Hypothesis H1b), while LPJ-GUESS shows a stronger sensitivity to drought intensity
 427 (Hypothesis H1a). ED2’s sensitivity to the duration of drought was mild at Palo Verde (Fig. 2a),
 428 and stronger at EucFACE particularly during the 4-year drought with a strong non-monotonic
 429 pattern (see explanation below) (Fig. 2b). When reporting only percentage of biomass loss, ED2
 430 predicts close to no UCE response at Palo Verde; with a maximum biomass reduction of only
 431 40% during 95% precipitation removal and a 4-year drought event (i.e., UCE). LPJ-GUESS
 432 shows **threshold tipping patterns** highly sensitive to drought intensity. C loss predicted by LPJ-

Deleted: n “integrated-C-change”

Deleted: integrated-C-loss

Deleted: integrated-C-loss

Integrated-C-change = *integrated C Loss_{drought}*

Deleted:

Formatted: Centered

Deleted: integrated-C-loss

Deleted: integrated-C-change

Deleted: reduced

Deleted: integrated-C-change

Deleted: reference

Deleted: to

Deleted: at both sites

Deleted: for biomass and LAI

Deleted: Both models had similar biomass compared to observations at Palo Verde (10.4 - 11.7 vs. 11.0 kgC m⁻²), and at EucFACE biomass matched well in LPJ-GUESS (12.1 vs. 12.7 kgC m⁻²) but was low in ED2 (5.6 kgC m⁻²). Both models also had similar LAI to observations at Palo Verde (3.3 - 4.5 vs. 3.8 (± 1.06) m² m⁻²), and at EucFACE LAI matched well in ED2 (1.6 vs. 1.7 m² m⁻²), but was high for LPJ-GUESS (3.2 m² m⁻²). At EucFACE LAI ranged from 1.2 to 2.1 over a 28-month measurement period (Duursma et al., (2016), but LPJ-GUESS had very large fluctuations in annual LAI outside of these ranges (Fig. S1).

Deleted: Both

Deleted: in concurrence with Hypothesis H1, but they

Deleted: very little sensitivity to drought duration but is

459 GUESS at Palo Verde reached a threshold at ~65% drought intensity, after which forests exhibit
460 strong biomass losses, up to 100% (Fig. 2a). At the EucFACE site, both models predict a critical
461 threshold of biomass loss at 35%-45% drought intensity, with LPJ-GUESS predicting total
462 biomass loss (up to 100%) after this drought intensity threshold (Fig. 2b). The EucFACE drought
463 threshold is lower than that of the seasonally dry mixed tropical forest in Palo Verde.

464 With respect to C loss over a recovering time period (~~severity-drought index~~), the two
465 models predict similar drought responses at Palo Verde (Fig. 2c), but not at EucFACE (Fig. 2d).
466 At Palo Verde, the similarity between models in ~~severity-drought index~~, reflected longer biomass
467 recovery time but less biomass loss in the short-term in ED2 relative to LPJ-GUESS, which
468 predicted greater biomass loss immediately after drought but shorter recovery time. With the
469 exception of the 1-year drought in ED2, both models predict similar ~~severity-drought index~~,
470 across a range of UCEs at Palo Verde, via different pathways. The ~~severity-drought index~~,
471 revealed an ~~exacerbated~~ response to drought duration in ED2 ~~with drought durations greater than~~
472 ~~one year~~ (Fig. 2c), ~~compared to~~ when only examining ~~loss~~ in biomass ~~at the time of the event~~
473 (Fig. 2a). The “V”-shaped patterns observed particularly in Fig. 2b, arise from interactions
474 between whole-leaf phenology and stomatal responses to drought in ED2. For drought intensities
475 lower than 40%, stomatal conductance is reduced but leaves are not fully shed. Leaf respiration
476 continues, gradually depleting non-structural C pools, followed by a loss of biomass. However,
477 for higher drought intensities, leaf water potentials quickly become systematically lower than
478 leaf turgor loss points and tree cohorts shed all their leaves. This strategy represents an
479 immediate loss of C via leaf shedding, but spares the cohort from slow, respiration-driven
480 depletion of C stocks.

482 3.1 Predicted model responses to UCE droughts combined with increased temperature 483 and/or eCO₂

484 Relating to our second hypothesis of additional effects of warming and eCO₂, we tested
485 15 treatments in total, repeating the five climate change scenarios for each of the three drought
486 durations. With the addition of climate change impacts, ED2 remained sensitive to the duration
487 of drought, with warming negatively impacting ~~severity-climate index~~ and most consistently
488 during 2- and 4-year drought durations. ED2 predicts that during the 2- and 4-year droughts at
489 EucFACE, losses are exacerbated when accompanied with warming, even with eCO₂, with 600

Deleted: integrated-C-loss

Deleted: integrated-C-loss

Deleted: integrated-C-loss

Deleted: integrated-C-loss metric

Deleted: strong nonlinear

Deleted: while this nonlinearity is less evident

Deleted: change

Deleted: integrated-C-change

498 ppm having a more detrimental impact than the more elevated 800 ppm (Fig. 3b-c). The average
499 severity-climate index was -111.0 kg C m⁻² yr across all 15 treatments (Table 2). Only during the
500 1-year drought duration did drought plus warming and eCO₂ have a buffering effect on C stocks,
501 seen in four out of our five scenarios but only during relatively modest droughts intensities (Fig.
502 3a; i.e., positive severity-climate index, see also Table 2).

503 The ED2 simulations of the seasonally dry Palo Verde site (Fig. 3d-f), produced less
504 frequent negative impacts on drought and climate change driven C losses compared to
505 EucFACE, with an average severity-climate index of -53.9 kg C m⁻² yr across all 15 treatments
506 (Table 2). During the 2-year drought, applying +2K with eCO₂ to 600 ppm showed a slight
507 buffering effect to droughts and the most consistent positive severity-climate index (Fig. 3e;
508 Table 2). Interestingly, an increase in only eCO₂ to 800 ppm (no warming) when applied with the
509 2- and 4-year droughts resulted in the largest loss in carbon (Fig. 3e-f), larger than the expected
510 'most severe' scenario; +2K and 800 ppm.

511 Similar to ED2, the LPJ-GUESS model showed a nearly complete negative response in
512 severity-climate index as a result of UCE drought and scenarios of warming and eCO₂ at the
513 EucFACE site (Fig. 3g-i), but mixed and more muted results at Palo Verde (Fig. 3j-l, Table 2).
514 The average severity-climate index relative to the no climate change control case was -95.4 at
515 EucFACE and -7.8 kg C m⁻² yr at Palo Verde, both less negative compared to ED2. One notable
516 pattern was up until a drought intensity threshold of ~40%, the climate scenarios had no effect or
517 response in severity-climate index at EucFACE, and the muted response from warming and
518 eCO₂ Palo Verde, compared to ED2. Surprisingly, the +2K scenario switched the severity-
519 climate index to positive, compared to the control case (Fig. 3g-i; red lines), potentially a
520 physiological process in the model to increased temperatures only that signals an anomalous
521 resiliency response. Similar to the results with no climate change, LPJ-GUESS remained
522 sensitive to the intensity of drought, with ~40% precipitation reduction being a threshold.

523 When comparing the VDM responses to increasing drought severity and its interactions
524 with warming and eCO₂ (related to conceptual Fig. 1d), ED2 showed a more consistent MO
525 response during UCEs and with additional warming and eCO₂ (Fig. 3; negative severity-climate
526 index), especially at EucFACE, suggesting these ecosystems will remain in a depressed carbon
527 condition driving vegetation mortality, and/or longer recoveries. LPJ-GUESS produced more
528 opportunities for SO with climate change. For example, at EucFACE CO₂ fertilization created

Deleted: integrated-C-change

Deleted:

Deleted: integrated-C-change

Deleted: integrated-C-change

Deleted: -1

Deleted: integrated-C-change

Deleted: integrated-C-change

Deleted: integrated-C-change

Deleted: integrated-C-change

Deleted: reference

Deleted: integrated-C-change

Deleted: integrated-C-change

Deleted: reference

Deleted: The models and sites differed with regard to SO and MO...

Deleted: .

Deleted:

Deleted: integrated-C-change

547 small SO periods that then led to MO with increasing drought severities, and at Palo Verde all
548 +2K and 600 ppm led to a SO (Fig. 3j-l; Table 2).

549 Both models predicted that C losses due to drought interactions with increased
550 temperature and eCO₂ were less severe at the seasonally dry Palo Verde site compared to the
551 somewhat less seasonal, more humid EucFACE site (Table 2), which could be attributed to
552 higher diversity in PFT physiology at Palo Verde. Palo Verde's community composition that
553 emerged following drought included either three (LPJ-GUESS) or four (ED2) PFTs, while only a
554 single PFT existed at EucFACE. With rising temperatures under climate change, UCEs will be
555 hotter and drier. Nine out of the twelve simulations with both +2K and 600 ppm CO₂, and all but
556 one +2K and 800 ppm CO₂ produced a negative severity-climate index, implying stronger C
557 losses and/or longer recovery times when droughts are exacerbated by increasing temperatures
558 (Table 2).

Deleted:

Deleted: integrated-C-change

560 4 Discussion

561 Vegetation demographic models (VDMs) allowed us to uniquely explore two hypotheses
562 regarding a range of modeled response of terrestrial ecosystems to unprecedented climate
563 extremes (UCEs), and setting the stage for the following perspectives to help guide future
564 research. Key model results indicate strong differences in nonlinearities in C response to extreme
565 drought intensities in LPJ-GUESS and alternatively drought durations in ED2 (at one of two
566 sites), with differences in thresholds between the two models and ecosystems, and only the ED2
567 model representing impacts from combined intensity and drought (Hypothesis H1c). These
568 nonlinearities may arise from multiple mechanisms that we begin to investigate here, including
569 shifts in plant hydraulics or other functional traits, C allocation, phenology, stand size-structure
570 and/or age demography, and compositional changes, all which vary among ecosystem types. A
571 critical look of driving model mechanisms, which emerged from the hypothetical drought
572 simulations used here, are summarized in Table 3. The models also show exacerbated biomass
573 loss and recovery times in the majority of our scenarios of warming and eCO₂, supporting
574 Hypothesis H2. Below, we discuss the underlying mechanisms that drive simulated ecosystem
575 response to UCEs using the models and sites as conceptual "experimental tools" and
576 observational evidence from the literature. We focus on two temporal stages of the UCE: The
577 pre-drought ecosystem stage characterized as the quasi-stable state of the ecosystem prior to a

Deleted: clude

Deleted: (Hypothesis H1)

582 UCE, which can mediate ecosystem resistance and disturbance impact, and the post-drought
583 recovery stage (Table 1).

584

585 **4.1 The role of ecosystem processes and states prior to UCEs**

586 **4.1.1 The role of phenology and phenological strategies prior to UCEs:**

587 Observations show that diversity of deciduousness contributes to successful alternative
588 strategies for tropical forest response to water stress (Williams et al., 2008). For example, during
589 the severe 1997 El Nino drought, brevi-deciduous trees and deciduous stem-succulents within a
590 tropical dry site in Guanacaste Costa Rica retained leaves during the extreme wet-season
591 drought, behaving differently than during normal dry seasons (Borchert et al., 2002). Both
592 models here predict that neither seasonal deciduousness, nor drought-deciduous phenology at the
593 seasonally dry tropical forest, Palo Verde (which consists of trees with different leaf
594 phenological strategies), act to buffer the forest from a large drop in LAI during UCEs (Fig. S1a-
595 b). Even with this large decrease in LAI, ED2 predicted a very weak biomass loss at the time of
596 UCEs (Fig. 2a), suggesting large-scale leaf loss is not a direct mechanism of plant mortality in
597 ED2. Leaf loss is one component of total carbon turnover flux equations in terrestrial models, in
598 addition to woody loss, fine-roots, and reproductive tissues. Having a better understanding of
599 when extreme levels of phenological turnover contribute to stand-level mortality could be
600 improved. Among other turnover hypothesis explored, Pugh et al. (2020) found that phenological
601 turnover fluxes were just as important as mortality fluxes in driving forest turnover time in the
602 VDMs: LPJ-GUESS, CABLE-POP, ORCHIDEE, but not the LSM JULES. At the EucFACE
603 site prior to the simulated extreme drought, LPJ-GUESS displayed strong inter-annual variability
604 in LAI (Fig. S1a-b). This capability of large swings in LAI (5.8 to 0.8) by LPJ-GUESS could
605 contribute to model uncertainty and the considerable mortality response at EucFACE. Modeled
606 LAI was the largest source of variability in another ecosystem model, CABLE, when evaluating
607 the simulated response to CO₂ fertilization (Li et al., 2018). VDMs could be improved by better
608 capturing different plant phenological responses to UCEs by better representing a range of leaf-
609 level morphological and physiological characteristics relevant to plant-water relations such as
610 leaf age, retention of young leaves even during extreme droughts, (Borchert et al., (2002)), and
611 variation in hydraulic traits as a function of leaf habit (Vargas et al., (2021)) (Table 3). Two such

612 examples are seen in the FATES model where the possibility for “trimming” the lowest leaf
613 layer can occur when leaves are in negative carbon balance due to light limitation thus
614 optimizing maintenance costs and carbon gain, as well as leaf age classifications providing
615 variations in leaf productivity and turnover.

616

617 **4.1.2 The role of plant hydraulics prior to UCEs:**

618 Susceptibility of plants to hydraulic stress is one of the strongest determinants of
619 vulnerability to drought, with loss of hydraulic conductivity being a major predictor of drought
620 mortality in temperate (McDowell et al., 2013; Anderegg et al., 2015; Sperry and Love, 2015;
621 Venturas et al., 2021) and tropical forests (Rowland et al., 2015; Adams et al., 2017b), as well as
622 a tractable mortality mechanism to represent in process-based models (Choat et al., 2018,
623 Kennedy et al., 2019). Both LPJ-GUESS and ED2 exhibited a wide range in amount and pattern
624 of plant-available-water prior to drought (Fig. S1c-d), contributing to large differences in UCE
625 response. LPJ-GUESS, which does not simulate hydrodynamics, predicted lower total plant-
626 available-water at both sites compared to ED2, and subsequently simulated greater mortality and
627 a greater increase in plant-available-water right after the UCEs as a result of less water demand.
628 Due to ED2 using a static mortality threshold from conductivity loss (88%), it likely does not
629 accurately reproduce the wide range of observations of drought-induced mortality. In ED2, large
630 trees, with longer distances to transport water, were at higher risk and suffered higher mortality
631 (Fig. 4), demonstrating how stand demography, size structure, and tapering of xylem conduits
632 can play an important role in ecosystem models (Petit et al., 2008; Fisher et al., 2018). Of the
633 VDMs that are beginning to incorporate a continuum of hydrodynamics (e.g., ED2 (described in
634 Methods 2.1 section) and FATES-HYDRO (Fang et al., 2022, based on Christoffersen et al.,
635 2016), they are able to solve for transient water from soils to roots, through the plant and connect
636 with transpiration demands. Therefore, instead of the plant water stress function being based on
637 soil water potentials, it is replaced with more realistic connections with leaf water potentials.
638 Mortality is then caused by hydraulic failure via embolism controlled by the critical water
639 potential (P_{50}) that leads to 50% loss of hydraulic conductivity. For advancements in tree level
640 hydrodynamic modeling see the FETCH3 model (Silva et al., 2022), for justification for plant
641 hydrodynamics in conjunction with multi-layer vertical canopy profiles see Bonan et al., (2021).
642 There are strong interdependencies and related mechanisms connecting both hydraulic failure

643 (e.g., low soil moisture availability) and C limitation (e.g., stomatal closure) during drought
644 (McDowell et al., 2008; Adams et al., 2017b), and these interactions should be incorporated in
645 ecosystem modeling and further explored (Table 3).

646 **4.1.3. The role of carbon allocation prior to UCEs:**

647 Plants have a variety of strategies to buffer vulnerability to water and nutrient stress
648 caused by extreme droughts, such as allocating more C to deep roots (Joslin et al., 2000; Schenk
649 and Jackson, 2005), investing in mycorrhizal fungi (Rapparini and Peñuelas, 2014), or reducing
650 leaf area without shifting leaf nutrient content (Pilon et al., 1996). Alternatively, presence of
651 deep roots doesn't necessarily lead to deep soil moisture utilization, as seen in a 6-year
652 Amazonian throughfall exclusion experiment where deep root water uptake was still limited,
653 even with high volumetric water content (Markewitz et al., 2010). Elevated CO₂ alone will
654 enhance growth and water-use efficiency (Keenan et al., 2013), reducing susceptibility to
655 drought. However, such increased productivity within a forest stand, and associated structural
656 overshoot during favorable climate windows, can also be reversed by increased competition for
657 light, nutrients, and water during unfavorable UCEs – potentially leading to mortality overshoot
658 (Fig. 1d) and higher C loss. Mortality overshoot, as a result of structural overshoot, could be an
659 explanation for the negative [severity-climate index](#) (i.e., C loss) in the majority of eCO₂-only
660 simulations (18 out of 24 scenarios; Table 2).

661 Effects of CO₂ fertilization on plant C allocation strategies are uncertain. As a result,
662 ecosystem models differ in their assumptions on controls of C allocation in response to eCO₂,
663 leading to divergent plant C use efficiencies (Fleischer et al., 2019). Global scale terrestrial
664 models are beginning to include optimal dynamic C allocation schemes, over fixed ratios, that
665 account for concurrent environmental constraints on plants, such as water, and adjust allocation
666 based on resource availability such as in LM3-PPA (Weng et al., 2015), but the representation of
667 C allocation is still debated and progressing (De Kauwe et al., 2014; Montané et al., 2017; Reyes
668 et al., 2017). Options for carbon allocation strategies can based on the allometric partitioning
669 theory (i.e., allocation follows a power allometry function between plant size and organs which
670 is insensitive to environmental conditions; Niklas, 1993), as an alternative to ratio-based optimal
671 partitioning theory (i.e., allocation to plant organs based on the most limiting resources)
672 (McCarthy and Enquist, 2007) or fixed ratios (Table 3), and the strategies should be further
673 investigated particularly due to VDMs substantial use of allometric relationships. A meta-

Deleted: integrated-C-change

675 analysis of 164 studies found that allometric partitioning theory outperformed optimal
676 partitioning theory in explaining drought-induced changes in C allocation (Eziz et al., 2017).
677 Further eco-evolutionarily-based approaches such as optimal response or game-theoretic
678 optimization, as well as entropy-based approaches are useful when wanting to simulate higher
679 levels of complexity (reviewed in Franklin et al. 2012). With more frequent UCEs and the need
680 for plants to reduce water consumption, a shift in the optimal strategy of allocation between
681 leaves and fine roots should change. The goal functions (e.g., fitness proxy) used in optimal
682 response modeling can account for these shifts in costs and benefits of allocation between all
683 organs (Franklin et al. 2009, 2012).

684

685 **4.1.4 The role of plant carbon storage prior to UCEs:**

686 Studies of neotropical and temperate seedlings show that pre-drought storage of non-
687 structural carbohydrates (NSCs) provides the resources needed for growth, respiration
688 osmoregulation, and phloem transport when stomata close during subsequent periods of water
689 stress (Myers and Kitajima, 2007; Dietze and Matthes, 2014; O'Brien et al., 2014). Furthermore,
690 direct correlations have been shown between NSC depletion and embolism accumulation, and
691 the degree of pre-stress reserves and utilization of soluble sugars (Tomasella et al., 2020). The
692 amount of NSC storage required to mitigate plant mortality during C starvation and interactions
693 with hydraulic failure from severe drought is difficult to quantify, due to the many roles of NSCs
694 in plant function and metabolism (Dietze and Matthes, 2014). For example, NSCs were not
695 depleted after 13 years of experimental drought in the Brazilian Amazon (Rowland et al., 2015).
696 As atmospheric CO₂ increases with climate change, NSC concentrations may increase, as seen in
697 manipulation experiments (Coley, 2002), but interactions with heat, water stress, enhanced leaf
698 shedding, and nutrient limitation complicates this relationship, and needs to be further explored.
699 Despite the recognition of the critical role that plant hydraulic functioning and NSCs play in tree
700 resilience to extremes, knowledge gaps and uncertainties preclude fully incorporating these
701 processes into ecosystem models.

702 Compared to ED2, LPJ-GUESS predicted low plant carbon storage (a model proxy for
703 NSCs) prior to and during drought, and at times became negative, thereby creating C costs (Fig.
704 S2a-b), leading to C starvation and potentially explaining the larger biomass loss in LPJ-GUESS
705 at both sites. Alternatively, ED2 maintained higher levels of NSCs providing a buffer to stress,

706 and mitigating the negative effects of drought. Maintenance of NSCs in ED2, even during
707 prolonged drought (at EucFACE) is due to: (1) trees resorbing a fraction of leaf C during leaf
708 shedding, (2) no maintenance costs for NSC storage in the current version, and (3) no allocation
709 of NSCs to structural growth until NSC storage surpasses a threshold (the amount of C needed to
710 build a full canopy of leaves and associated fine roots), allowing for a buffer to accumulate. In
711 LPJ-GUESS, accumulation and depletion of NSC is recorded as a 'C debt' being paid back in
712 later years. The contrasting responses of the two models to drought, and the likely role of NSCs
713 in explaining differences in model behavior, highlights the need to better understand NSC
714 dynamics and to accurately represent the relevant processes in models (Richardson et al., 2013;
715 Dietze and Matthes, 2014). More observations of C accumulation patterns and how/where NSCs
716 drive growth, respiration, transport and cellular water relations would enable a more realistic
717 implementation of NSC dynamics in models (Table 3).

718

719 **4.1.5 Role of functional trait diversity prior to UCEs:**

720 Currently LPJ-GUESS simulates the Palo Verde community using three PFTs, while ED2 uses
721 four PFTs that differ in photosynthetic and hydraulic traits. The community composition simulated by
722 ED2 is shown to be more resistant to UCEs compared to LPJ-GUESS (Fig. 5), perhaps due to
723 relatively higher functional diversity (via more PFTs with additional phenological and hydraulic
724 diversity). This additional diversity helps to buffer ecosystem response to drought by allowing more
725 tolerant PFTs to benefit from reductions in less-tolerant PFTs, thus buffering reductions in ecosystem
726 function (Anderegg et al., 2018). Higher diversity ecosystems were found to protect individual species
727 from negative effects of drought (Aguirre et al., 2021) and enhance productivity resilience following
728 wildfire (Spasojevic et al., 2016); thus, functionally diverse communities may be key to enhancing
729 tolerance to rising environmental stress.

730 Recent efforts to consolidate information on plant traits (Reich et al., 2007; Kattge et al., 2011)
731 have contributed to identifying relationships that can impact community-level drought responses
732 (Skelton et al., 2015; Anderegg et al., 2016a; Uriarte et al., 2016; Greenwood et al., 2017), such as
733 life-history characteristics, and strategies of resource acquisition and conservation as predictors of
734 ecosystem resistance (MacGillivray et al., 1995; Ruppert et al., 2015). While adding plant trait
735 complexity in ESMs may be required to accurately simulate key vegetation dynamics, it necessitates
736 more detailed parameterizations of processes that are not explicitly resolved (Luo et al., 2012). Further

737 investigation of how VDMs represent interactions leading to functional diversity shifts is crucial to
738 this issue. Enquist and Enquist, (2011), as an example, show that long-term patterns of drought (20-
739 years) have led to increases in drought-tolerant dry forest species, which could modulate resistance to
740 future droughts. Higher diversity of plant physiological traits and drought-resistance strategies is
741 expected to enhance community resistance to drought, and models should account for shifts in diverse
742 functionality (Table 3).

743

744 **4.2 The role of ecosystem processes and states in post-UCE recovery**

745 **4.2.1 The role of soil water resources post-UCES:**

746 Our simulation results generally demonstrated a fast recovery of plant-available-water
747 and LAI at both sites (Fig. S1). Annual plant-available-water substantially increased right after
748 drought by an average of 163 mm at Palo Verde and 213 mm at EucFACE in the LPJ-GUESS
749 simulations, compared to much lower increases in ED2 (50 mm and 12 mm at Palo Verde and
750 EucFACE). This increase in available water post-drought can be attributed to reduced stand
751 density and water competition (Fig. S2c-d; diamonds vs. circles), alleviating the demand for soil
752 resources (water) and subsequent stress, which has also been shown in observations (McDowell
753 et al., 2006; D'Amato et al., 2013). After large canopy tree mortality events there can be
754 relatively rapid recovery of forest biogeochemical and hydrological fluxes (Biederman et al.,
755 2015; Anderegg et al., 2016b; Biederman et al., 2016). These crucial fluxes strongly influence
756 plant regeneration and regrowth, which can buffer ecosystem vulnerability to future extreme
757 droughts. However, this enhanced productivity has a limit. In a scenario where UCES continue to
758 intensify, causing greater reductions in soil water and reduced ecosystem recovery potential, the
759 SO growth that typically occurs after UCES may be dampened (Fig. 1d). In water-limited
760 locations, similar to the dry forest sites used here, initial forest recovery from droughts were
761 faster due to thinning induced competitive-release of the surviving trees, and shallow roots not
762 having to compete with neighboring trees for water, allowing for more effective water user
763 (Tague and Moritz, 2019), stressing the importance of root competition and distribution in
764 models (Goulden and Bales, 2019). Tague and Moritz, (2019) also reported that this increased
765 water use efficiency and SO ultimately lead to water stress and related declines in productivity,
766 similar to the MO concept (Jump et al., 2017; McDowell et al., 2006). Since a core strength of

767 VDMs is predicting stand demography during recovery, improved quantification of density-
768 dependent competition following stand dieback would be beneficial for model benchmarking
769 (Table 3).

770

771 **4.2.2 The role of lagged turnover and secondary stressors post-UCEs:**

772 Time lags in forest compositional response and survival to drought could indicate
773 community resistance or shifts to more competitive species and competitive exclusion. During a
774 15-year recovery period from extreme drought at Palo Verde, LPJ-GUESS predicted an increase
775 in stem density (stems $\text{m}^2 \text{yr}^{-1}$) (Fig. S2c) compared to ED2, which predicted almost no impact in
776 stem recovery. The mortality “spike” in ED2 due to drought was muted and slightly delayed,
777 contributing to ED2’s lower biomass loss and more stable behavior of plant processes over time
778 at Palo Verde. At EucFACE, both models exhibited a pronounced lag effect in stem turnover
779 response, i.e. ~8-12 years after drought (Fig. S2d). After about a decade, strong recoveries and
780 increased stem density occurred, which in ED2 was followed by delayed mortality/thinning of
781 stems. Delayed tree mortality after droughts is common due to optimizing carbon allocation and
782 growth (Trugman et al., 2018), but typically only up to several years post-drought, not a decade
783 or more as seen in the model.

784 The versions of the VDMs used here do not directly consider post-drought secondary
785 stressors such as infestation by insects or pathogens, and the subsequent repair costs due to stress
786 damage, which could substantially slow the recovery of surviving trees. Forest ecologists have
787 long recognized the susceptibility of trees under stress, particularly drought, to insect attacks and
788 pathogens (Anderegg et al., 2015). Tight connections between drought conditions and increased
789 mountain pine beetle activity have been observed (Chapman et al., 2012; Creeden et al., 2014),
790 and can ultimately lead to increased tree mortality (Hubbard et al., 2013). Leaf defoliation is a
791 major concern from insect outbreaks following droughts, and can have large impacts on C
792 cycling, plant productivity, and C sequestration (Amiro et al., 2010; Clark et al., 2010; Medvigy
793 et al., 2012). Implementing these secondary stressors in models could slow the rate of post-UCE
794 recovery and lead to increased post-UCEs tree mortality.

795

796 **4.2.3 The role of stand demography post-UCEs:**

797 Change in stand structure is an important model process to capture, because large trees
798 have important effects on C storage, community resource competition, and hydrology
799 (Wullschleger et al., 2001) (Table 3), and maintaining a positive carbohydrate balance is
800 beneficial in sustaining (or repairing) hydraulic viability (McDowell et al., 2011). There is
801 increasing evidence, both theoretical (McDowell and Allen, 2015) and empirical (Bennett et al.,
802 2015; Rowland et al., 2015; Stovall et al., 2019), that large trees (particularly tall trees with high
803 leaf area) contribute to the dominant fraction of dead biomass after drought events. Under rising
804 temperatures (and decreasing precipitation), VPD will increase, leading to a higher likelihood of
805 large tree death (Eamus et al., 2013; Stovall et al., 2019), driving MO events as hypothesized in
806 Fig. 1d. Consistent with this expectation, ED2 predicted that the largest trees (>100 cm)
807 experienced the largest decreases in basal area to compared to all other size classes (Fig. 4). This
808 drought-induced partial dieback and mortality of large dominant trees has substantial impacts on
809 community-level C dynamics, as long-term sequestered C is liberated during the decay of new
810 dead wood (Palace et al., 2008; Potter et al., 2011). In ED2, the intermediate size class (60 - 80
811 cm) increased in basal area following large-tree death, taking advantage of the newly open
812 canopy space. However, small size classes do not necessarily benefit from canopy dieback. For
813 example, in a dry tropical forest, prolonged drought led to a decrease in understory species and
814 small-sized stems (Enquist and Enquist, 2011).

815 Due to VDMs being able to exhibit dynamic biogeography they are more useful at
816 predicting shifts in community composition beyond LSMs capabilities. Further areas of
817 advancement (described in Franklin et al. (2020)) is including models of natural selection, self-
818 organization, and entropy maximization which can substantially improve community dynamic
819 responses in varying environments such as UCEs. Eco-evolutionary optimality (EEO) theory can
820 also help improve functional trait representation in global process-based models (reviewed in
821 Harrison et al., 2021), through hypotheses in plant trait trade-offs and mechanistic links between
822 processes such as resource demand, acquisition, and plant's competitiveness and survival; traits
823 associated with high degrees of sensitivity in models. The power of prognostic VDMs to predict
824 shifts in demography and community migration with climate change is large, but rarely is being
825 constrained with plant-level EEO theory, and thus will likely need to use stand level competition
826 and coexistence principles of how plants self-organize (Franklin et al. 2020).

827

828 **4.2.4 The role of functional trait diversity & plant hydraulics post-UCEs:**

829 In field experiments, higher disturbance rates have shifted the recovery trajectory and
830 competition of the plant community towards one that is composed of opportunistic, fast-growing
831 pioneer tree species, grasses (Shiels et al., 2010; Carreño-Rocabado et al., 2012), and/or
832 deciduous species, as also seen in model results (Hickler et al., 2004). In the treatments presented
833 here, deciduous PFT types were also the strongest to recover after 15 years in both models,
834 surpassing pre-drought values (Fig. 5). It should be noted that ED2 exhibited a strong recovery in
835 the evergreen PFT as well, inconsistent with the above literature (Fig. 5b). PFTs in ED2 respond
836 to drought conditions via stomatal closure and leaf shedding, buffering stem water potentials
837 from falling below a set mortality threshold (i.e., 88% of loss in conductivity). This conductivity
838 threshold may need to be reconsidered if further examination reveals an unrealistic advantage
839 under drought conditions for evergreen trees, which exhibited a lower impact from droughts
840 (compared to deciduous and brevi-deciduous PFTs) in ED2. Nitrogen cycling feedbacks were
841 not investigated here, but could also be an explanation for a strong evergreen PFT recovery.

842 Recovery of surviving trees could be hindered by the high cost of replacing damaged
843 xylem associated with cavitation (McDowell et al., 2008; Brodribb et al., 2010). Many studies
844 have identified “drought legacy” effects of delayed growth or gross primary productivity
845 following drought (Anderegg et al., 2015; Schwalm et al., 2017) and the magnitude of these
846 legacies across species correlates with the hydraulic risks taken during drought itself (Anderegg
847 et al., 2015). The conditions under which xylem can be refilled remain controversial, but it seems
848 likely that many species, particularly gymnosperms, may need to entirely replace damaged
849 xylem (Sperry et al., 2002), and trees worldwide operate within narrow hydraulic safety margins,
850 suggesting that trees in all biomes are vulnerable to drought (Choat et al., 2012). The amount of
851 damaged xylem from a given drought event and recovery rates also vary across trees of different
852 sizes (Anderegg et al., 2018).

853 Plasticity in nutrient acquisition traits, intraspecific variation in plant hydraulic traits
854 (Anderegg et al., 2015), and changes in allometry (e.g., Huber values) can have large effects on
855 acclimation to extreme droughts. This suggests some capacity for physiological adaptation to
856 extreme drought, as seen by short-term negative effects from drought and heat extremes being

857 compensated for in the longer term (Dreesen et al., 2014). Still, given the shift towards more
858 extreme droughts with climate change, vegetation mortality thresholds are likely to be exceeded,
859 as reported in Amazonian long-term plots where mortality of wet-affiliated genera has increased
860 while simultaneously new recruits of dry-affiliated genera are also increasing (Esquivel-Muelbert
861 et al., 2019). Increasing occurrences of heat events, water stress and high VPD will lead to
862 extended closure of stomata to avoid cavitation, progressively reducing CO₂ enrichment benefits
863 (Allen et al., 2015). Where CO₂ fertilization has been seen to partially offset the risk of
864 increasing temperatures, the risk response was mediated by plant hydraulic traits (Liu et al.,
865 2017) using a soil–plant–atmosphere continuum (SPAC) model, yet interactions with novel
866 extreme droughts were not considered. The VDM simulations suggest that the combination of
867 elevated warming and potential structural overshoot from eCO₂ (or inaccurate representation in
868 NSCs allocation/usage priority) will exacerbate consequences of UCEs by reductions in both C
869 stocks and post-drought biomass recovery speeds (Fig. 3). Therefore, future UCE recovery may
870 not be easily predicted from observations of historical post-disturbance recovery. An associated
871 area for further investigation is to better understand the hypothesized interplay between
872 amplified mortality from hotter UCEs followed by structural overshoot regrowth during wetter
873 periods (Fig. 1d), which could potentially lead to continual large swings in MO and SO and
874 vulnerable net ecosystem C fluxes through time (Table 3).

875

876 **5 Summary of perspectives for model advancement**

877 Model limitations and unknowns exposed by our simulations and literature review
878 highlight current challenges in our ability to understand and forecast UCE effects on ecosystems.
879 These limitations reflect a general lack of empirical experiments focused on UCEs. Insufficient
880 data means that relevant processes may currently be poorly represented in models, and models
881 may then misrepresent C losses during UCEs. The two VDMs used here had different
882 sensitivities to drought duration or intensity, and CO₂ and warming interactions, indicating the
883 wide variety of unknowns and plausible options when trying to represent future UCEs that still
884 needs to be narrowed down (Fig. 1d). These model uncertainties could potentially be addressed
885 by improved datasets on thresholds of conductivity loss at high drought intensities, the role of
886 trait diversity (e.g., different strategies of drought deciduousness and EEO theory) in buffering
887 ecosystem drought responses, and a better grasp of allocation to plant C storage stocks before,

Deleted: and

889 during, and after multi-year droughts. Our study takes some initial steps to identify and assess
890 model gaps in terms of mechanisms and magnitudes of responses to UCEs, which can then be
891 used to inform and develop field experiments targeting key knowledge gaps as well as to
892 prioritize ongoing model development (Table 3). Our intention was not to do an exhaustive list
893 of UCE simulation experiments, and additional modeling perturbations and experiments would
894 be useful outcomes of future studies. For example, we begin to investigate duration of droughts
895 but we did not consider frequency of back-to-back UCEs. Using VDMs as hypothesis testing
896 tools offers strong potential to drive progress in improving our understanding of terrestrial
897 ecosystem responses to UCEs and climate feedbacks, while informing the development of the
898 next generation of models.

Deleted: This iterative model-experiment framework of u

900 *Code Availability.* The source code for the ED2 model can be downloaded and available publicly
901 at <https://github.com/EDmodel/ED2>. The source code for the LPJ-GUESS model can be
902 downloaded and available publicly at <http://web.nateko.lu.se/lpj-guess/download.html>. All model
903 simulation data will be available in a Dryad repository.
904

905 *Data Availability.* Authors received the required permissions to use the site level meteorological
906 data used in this study. Otherwise, no ecological or biological data were used in this study.
907

908 *Author Contributions.* JH wrote the manuscript with significant contributions from AR, BS, JD,
909 DM, with input and contributions from all authors. XX and MM were the primary leads running
910 the model simulations, with model assistance and strong feedback from DM and BS. All authors
911 made contributions to this article, and agree to submission.
912

913 *Competing Interests.* The contact author has declared that neither they nor their co-authors have
914 any competing interests.
915

916 *Special Issue Statement.* Special Issue titled “Ecosystem experiments as a window to future
917 carbon, water, and nutrient cycling in terrestrial ecosystems”
918

919 *Financial Support:* Funding for the meetings that facilitated this work was provided by NSF-
920 DEB-0955771: An Integrated Network for Terrestrial Ecosystem Research on Feedbacks to the
921 Atmosphere and Climate (INTERFACE): Linking experimentalists, ecosystem modelers, and
922 Earth System modelers, hosted by Purdue University; as well as Climate Change Manipulation
923 Experiments in Terrestrial Ecosystems: Networking and Outreach (COST action ClimMani –
924 ES1308), led by the University of Copenhagen. J.A. Holm’s time was supported as part of the
925 Next Generation Ecosystem Experiments-Tropics, funded by the U.S. Department of Energy,
926 Office of Science, Office of Biological and Environmental Research under Contract DE-AC02-
927 05CH11231. AR acknowledges funding from CLIMAX Project funded by Belmont Forum and
928 the German Federal Ministry of Education and Research (BMBF). BS and MM acknowledge
929 support from the Strategic Research Area MERGE. W.R.L.A. acknowledges funding from the
930 University of Utah Global Change and Sustainability Center, NSF Grant 1714972, and the
931 USDA National Institute of Food and Agriculture, Agricultural and Food Research Initiative
932 Competitive Programme, Ecosystem Services and Agro-ecosystem Management, grant no. 2018-
933 67019-27850. JL acknowledges support from the Northern Research Station of the USDA Forest
934 Service (agreement 16-JV-11242306-050) and a sabbatical fellowship from sDiv, the Synthesis
935 Centre of iDiv (DFG FZT 118, 202548816). CDA acknowledges support from the USGS Land
936 Change Science R&D Program.
937

938 *Acknowledgements.* We thank Belinda Medlyn and David Ellsworth of the Hawkesbury Institute
939 for the Environment, Western Sydney University, for providing the meteorological forcing data
940 series for the EucFACE site, a facility supported by the Australian Government through the
941 Education Investment Fund and the Department of Industry and Science, in partnership with
942 Western Sydney University.
943

944 **Table 1.** Hypothesized plant processes and ecosystem state variables affecting pre-drought
945 resistance and post-drought recovery in the context of unprecedented climate extremes (UCEs).
946 The “Included in Model?” column indicates which processes or state variables are represented in
947 each of the two models studied in this paper. The mechanisms listed in the two right columns
948 refer to real-world ecosystems and are not necessarily represented in the ED2 and LPJ-GUESS
949 models. Contents of the table are based on a non-exhaustive literature review, expert knowledge,
950 and modeling results presented here. Symbols refer to the following literature sources: *
951 Borchert et al., 2002; Williams et al., (2008); ** Dietze and Matthes, (2014); O’Brien et al.,
952 2014; *** ENQUIST and ENQUIST, (2011); Greenwood et al., (2017); Powell et al., (2018); ^
953 Rowland et al., (2015); McDowell et al., (2013); Anderegg et al., (2015); ^^ Joslin et al., 2000;
954 Markewitz et al., (2010); ^^ Powell et al., (2018); ^^ Bennett et al., (2015); Rowland et al.,
955 (2015); ~ Hubbard et al., (2013); ~ ~ McDowell et al., (2006); D’Amato et al., (2013); + Zhu et
956 al., (2018); Vargas et al., (2021); % Trugman et al., (2019); %% Franklin et al., (2012); %%
957 Franklin et al., (2020).

Process or State Variable	Included in model?	Mechanisms affecting pre-UCE drought resistance influencing impact	Mechanisms affecting post-UCE drought recovery
Processes			
1) Phenology Schemes	ED2: Yes LPJ-G: Yes	- Leaf area and metabolic activity modulates vulnerability to death - Drought-deciduousness reduces vulnerability to drought *, with higher water potential at turgor loss point and less leaf vulnerability to embolism +	- Leaf lifespan tends to increase from pioneer to late-successional species in some ecosystems (e.g., tropical forests) and is a balance between C gain and its cost
2) Plant Hydraulics	ED2: Yes LPJ-G: No	- Cavitation resistance traits ^ - Turgor loss, hydraulic failure (stem embolism) lead to increased plant mortality and enhanced vulnerability to secondary stressors.	- Replacement cost of damaged xylem slows recovery of surviving trees
3) Dynamic Carbon Allocation	ED2: Yes LPJ-G: Yes	- Increased root allocation could offset soil water deficit under gradual onset of drought ^^ - Leaf C allocation strategies should be connected to hydraulic processes %	- Allocation among fine roots, xylem, & leaves affects recovery time & GPP/LAI trajectory - Eco-evolutionary optimality theory %%

4) Non-Structural Carbohydrate (NSC) Storage	ED2: Yes LPJ-G: Yes	- NSCs buffer C starvation mortality due to reduced primary productivity. - Maintenance of hydraulic function & avoiding hydraulic failure **	- Low NSC could increase vulnerability to secondary stressors during recovery
State Variables			
1) Plant-Soil Water Availability	ED2: Yes LPJ-G: Partly	- Low soil water potential increases risk of tree C starvation, turgor loss and hydraulic failure	- After stand dieback reduced demand for soil resources &/or reduced shading - Increased soil water enhances regeneration/ regrowth, buffers vulnerability to long-term drought ~ ~
2) Plant Functional Diversity	ED2: Yes LPJ-G: Yes	- Presence of drought-tolerant species modulates resistance at community level. - Shallow-rooting species more vulnerable ^^ ***	- Changed resource spectra shift competitive balance in favor of grasses and pioneer trees
3) Stand Demography	ED2: Yes LPJ-G: Yes	- Larger tree size enhances vulnerability to drought and secondary stressors due to higher maintenance costs ^^ ^^	- Mortality of canopy individuals favors understory species and smaller size-classes - Self-organizing principles %%%
4) Compounding Stressors	ED2: No LPJ-G: No	- Reduced resistance to insects and pathogens due to physiological/mechanical/ hydraulic damage & depletion of NSC	- Infestation by insects and pathogens, repair of damage due to secondary stressors, slows recovery of surviving trees ~

959 **Table 2** Impact of eCO₂ and/or temperature on the **severity-climate index** (kg C m⁻² yr) relative
 960 to drought treatments with no additional warming or eCO₂, for both models, and both sites seen
 961 in Fig. 3. Quantified as average and minimum **severity-climate index** across all 20 drought
 962 intensities for step-change scenarios of warming and eCO₂. The percentage of each scenario that
 963 was negative in **severity-climate index** (i.e., decreases in C-loss). Green values represent positive
 964 **severity-climate index**.

Deleted: integrated-C-change

Deleted: integrated-C-change

Deleted: integrated-C-change

Deleted:

Deleted: integrated-C-change

	<i>EucFACE</i>	<i>ED2</i>			<i>LPJ-GUESS</i>		
		Average severity-climate index	Largest severity-climate index	% climate scenario was negative	Average severity-climate index	Largest severity-climate index	% climate scenario was negative
1 year	600 ppm	2.2	0.0	33.3	-74.6	-396.6	36.8
	800 ppm	-10.6	-73.0	50.0	-124.1	-416.0	57.9
	2K	2.3	-0.5	16.7	21.3	-20.8	15.8
	2K, 600 ppm	0.5	-8.2	61.1	-67.5	-201.5	78.9
2 year	2K, 800 ppm	1.8	-0.4	22.2	-145.9	-400.1	47.4
	600 ppm	-105.6	-456.7	77.8	-85.2	-260.6	63.2
	800 ppm	-199.0	-522.9	83.3	-106.3	-350.1	42.1
	2K	-10.3	-34.7	77.8	14.2	-35.2	31.6
4 year	2K, 600 ppm	-204.9	-666.1	77.8	-47.6	-128.8	84.2
	2K, 800 ppm	-12.4	-61.6	50.0	-167.0	-421.9	68.4
	600 ppm	-125.5	-306.2	83.3	-122.6	-277.4	94.7
	800 ppm	-277.1	-423.3	100.0	-212.2	-523.7	89.5
	2K	-61.8	-188.6	72.2	12.9	-13.8	31.6
	2K, 600 ppm	-385.9	-674.2	94.4	-79.1	-197.3	94.7
	2K, 800 ppm	-277.9	-737.7	72.2	-247.0	-503.8	100.0
	Average	-111.0	-277.0	64.8	-95.4	-276.5	62.5
	<i>Palo Verde</i>	<i>ED2</i>			<i>LPJ-GUESS</i>		
1 year	600 ppm	-1.6	-6.2	77.8	-11.0	-32.4	78.9
	800 ppm	6.7	-0.2	11.1	-39.2	-154.0	100.0
	2K	-1.0	-15.3	38.9	-33.4	-75.1	100.0
	2K, 600 ppm	2.5	-1.1	22.2	6.5	-4.6	52.6
2 year	2K, 800 ppm	-6.6	-16.6	77.8	-121.1	-237.7	100.0
	600 ppm	15.1	-16.7	38.9	27.3	-6.0	10.5
	800 ppm	-229.2	-756.6	66.7	20.6	-17.2	26.3
	2K	-8.2	-71.8	50.0	32.0	-12.7	15.8
4 year	2K, 600 ppm	24.8	-5.7	11.1	36.2	-1.2	5.3
	2K, 800 ppm	-152.9	-348.1	77.8	8.0	-54.5	36.8
	600 ppm	-11.1	-37.3	94.4	3.4	-25.1	26.3
	800 ppm	-260.2	-694.8	94.4	-25.2	-132.6	57.9
	2K	-39.0	-133.8	66.7	-7.7	-45.9	68.4
	2K, 600 ppm	1.0	-16.4	38.9	6.1	-4.1	31.6
	2K, 800 ppm	-148.5	-429.3	83.3	-20.0	-75.5	78.9
	Average	-53.9	-170.0	56.7	-7.8	-58.6	52.6

	<i>EucFACE</i>	Average severity-climate index	Largest severity-climate index	% climate scenario was negative	Average severity-climate index	Largest severity-climate index	% climate scenario was negative
	800 ppm	-10.6	-73.0	50.0	-124.1	-416.0	57.9
	2K	2.3	-0.5	16.7	21.3	-20.8	15.8
	2K, 600 ppm	0.5	-8.2	61.1	-67.5	-201.5	78.9
	2K, 800 ppm	1.8	-0.4	22.2	-145.9	-400.1	47.4
2 year	600 ppm	-105.6	-456.7	77.8	-85.2	-260.6	63.2
	800 ppm	-199.0	-522.9	83.3	-106.3	-350.1	42.1
	2K	-10.3	-34.7	77.8	14.2	-35.2	31.6
	2K, 600 ppm	-204.9	-666.1	77.8	-47.6	-128.8	84.2
	2K, 800 ppm	-12.4	-61.6	50.0	-167.0	-421.9	68.4
4 year	600 ppm	-125.5	-306.2	83.3	-122.6	-277.4	94.7
	800 ppm	-277.1	-423.3	100.0	-212.2	-523.7	89.5
	2K	-61.8	-188.6	72.2	12.9	-13.8	31.6
	2K, 600 ppm	-385.9	-674.2	94.4	-79.1	-197.3	94.7
	2K, 800 ppm	-277.9	-737.7	72.2	-247.0	-503.8	100.0
	Average	-111.0	-277.0	64.8	-95.4	-276.5	62.5
	<i>Palo Verde</i>	<i>ED2</i>			<i>LPJ-GUESS</i>		
1 year	600 ppm	-1.6	-6.2	77.8	-11.0	-32.4	78.9
	800 ppm	6.7	-0.2	11.1	-39.2	-154.0	100.0
	2K	-1.0	-15.3	38.9	-33.4	-75.1	100.0
	2K, 600 ppm	2.5	-1.1	22.2	6.5	-4.6	52.6
	2K, 800 ppm	-6.6	-16.6	77.8	-121.1	-237.7	100.0
2 year	600 ppm	15.1	-16.7	38.9	27.3	-6.0	10.5
	800 ppm	-229.2	-756.6	66.7	20.6	-17.2	26.3
	2K	-8.2	-71.8	50.0	32.0	-12.7	15.8
	2K, 600 ppm	24.8	-5.7	11.1	36.2	-1.2	5.3
	2K, 800 ppm	-152.9	-348.1	77.8	8.0	-54.5	36.8
4 year	600 ppm	-11.1	-37.3	94.4	3.4	-25.1	26.3
	800 ppm	-260.2	-694.8	94.4	-25.2	-132.6	57.9
	2K	-39.0	-133.8	66.7	-7.7	-45.9	68.4
	2K, 600 ppm	1.0	-16.4	38.9	6.1	-4.1	31.6
	2K, 800 ppm	-148.5	-429.3	83.3	-20.0	-75.5	78.9
	Average	-53.9	-170.0	56.7	-7.8	-58.6	52.6

Deleted:

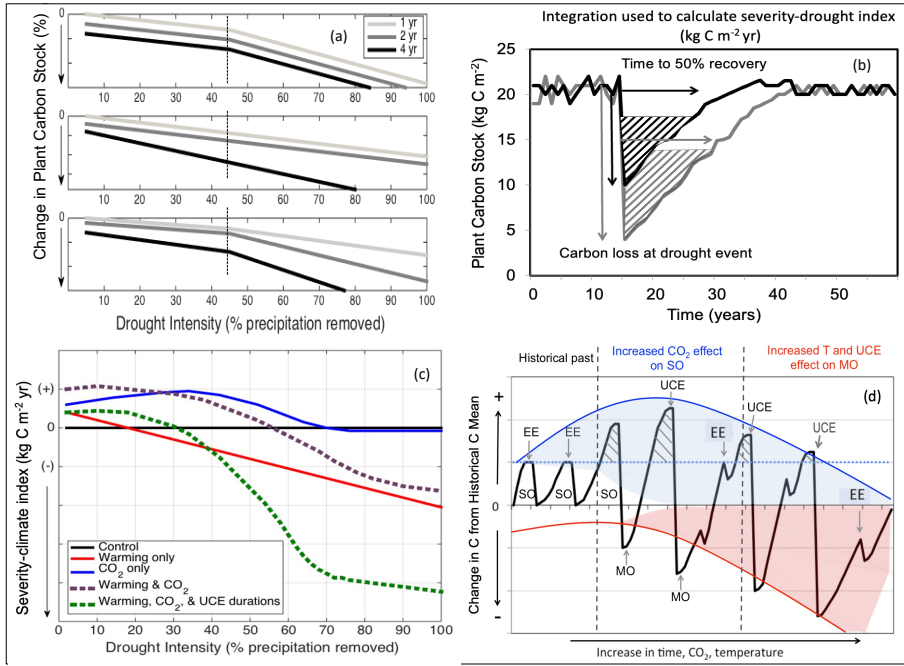
965

972 **Table 3** Summary of suggested critical look of driving mechanisms (e.g., ecosystem or plant
 973 processes and state variables) which emerged from the hypothetical drought simulations used
 974 here to explore for future research in manipulation experiments, data collection, and model
 975 development and testing, as related to furthering our understanding of UCE resistance and
 976 recovery.

UCE Drought Resistance & Recovery Summary	
Processes	Suggestions of driving mechanisms to further explore in data and models
1) Phenology Schemes	Represent morphological and physiological traits relevant to plant-water relations; drought- deciduousness can reduce vulnerability to drought; phenology of evergreens needs more investigation.
2) Plant Hydraulics	Interactions between hydraulic failure (e.g. low soil moisture availability) and C limitation (e.g. stomatal closure) during drought should be included in models. Account for turgor loss, hydraulic failure traits, costs to recover damaged xylem.
3) Dynamic Carbon Allocation	C allocation based on eco-evolutionary optimality (EEO) and allometric partitioning theory in addition <u>to</u> , or replacing ratio-based optimal partitioning theory, and fixed <u>allocation</u> ratios. Explore root allocation that could offset soil water deficits.
4) Non-structural Carbohydrate (NSC) Storage	Deciding best practices for NSC representation in models. Better understanding of NSC storage required to mitigate plant mortality during C starvation and interactions with avoiding hydraulic failure during severe droughts.
States Variables	
1) Plant-Soil Water Availability	Better quantification of the amount and accessibility of plant-available water for surviving trees, and tradeoff between increased structural productivity but vulnerability to subsequent droughts. Future relevance, or benefit, of lower water demand due to thinning with UCEs.
2) Plant Functional Diversity	Understand how higher diversity of plant physiological traits and drought-resistance strategies will enhance community resistance to drought; models still need to account for shifts in diverse functionality, including deciduousness shifts and interplay of regrowth structural overshoot followed by amplified mortality from hotter UCEs.
3) Stand Demography	Large trees more vulnerable to drought; need data on changes in C stock with UCEs in high-density smaller tree stands vs. stands with larger trees. Using 'self-organization' principles for modeling stand level competition and coexistence under UCEs.

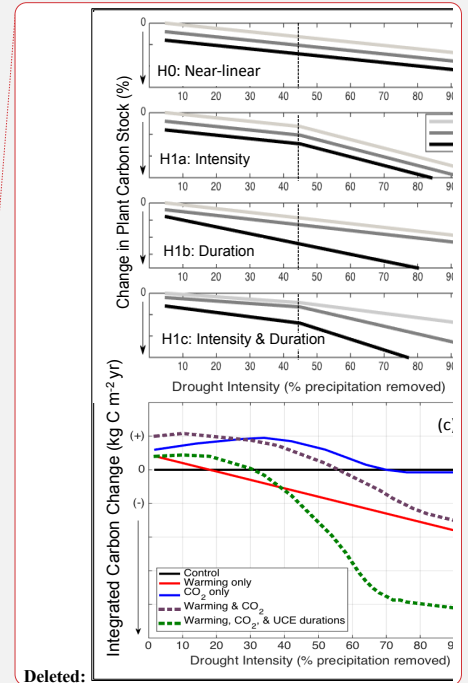
977

978



979

980 **Figure 1** Conceptual diagrams showing impacts of extreme droughts (unprecedented climate
 981 extremes, UCEs; i.e., record-breaking droughts) on plant C stocks. (a) **Conceptual diagram of**
 982 **UCE C loss:** potential loss in C stock as a function of increasing drought intensity (0-100%
 983 precipitation removal) and drought duration (1, 2 or 4 years of drought). In this example, an
 984 arbitrary threshold of 45% precipitation reduction and 4-year drought duration is assumed to
 985 correspond to a UCE. Hypotheses include nonlinear and threshold responses to drought intensity
 986 (H1a), drought duration via different slope responses (H1b), and combined effects of both
 987 drought intensity and durations (H1c). (b) **Conceptualized diagram of integrated C change:**
 988 responses of forest C stocks to a large (grey) and small (black) UCE. “Severity-drought index”
 989 (kg C m⁻² yr) denotes the integral of the C loss over time and is calculated from the two arrows:
 990 the total loss in C (kg C m⁻²) due to drought, and the time (yr) to recover 50% of the pre-drought
 991 C stock. (c) **Conceptualized UCE-climate C change diagram:** hypothetical response in
 992 terrestrial “severity-climate index” (kg C m⁻² yr) due to eCO₂ (blue line), rising temperature (red
 993 line), interaction between eCO₂ and temperature (dashed purple), and combined interactions



Deleted:

Deleted: response

Deleted: The “null hypothesis” (H0, top panel) is a near-linear response of C stocks to droughts. Alternative

Deleted: h

Deleted: UCE C loss

Deleted: Integrated-C-loss

Deleted: integrated-C-change

1002 among eCO₂, temperature, and UCEs of prolonged durations (green line), all relative to a
1003 reference drought of normal duration with no warming (black line). Severity-climate index
1004 denotes the difference in severity-drought index (see panel b) between a scenario of changing
1005 climatic drivers and the reference drought with no climate change (control). (d) **Conceptual**
1006 **UCE amplification diagram**: hypothetical amplified change in forest C stocks to eCO₂ and
1007 temperature relative to the pre-warming historical past (based on Jump et al. (2017)). Change in
1008 C stock greater than zero indicates a ‘structural overshoot’ (SO) due to favorable environmental
1009 conditions and/or recovery from an extreme drought-heat event (EE). Hashed black areas
1010 indicate a structural overshoot due to eCO₂, which occurs over the historical CO₂ levels (dashed
1011 blue line). Initially, an eCO₂ effect leads to a larger increase in structural overshoot (due to CO₂
1012 fertilization), driving more extreme vegetation mortality (‘mortality overshoot’ - MO) relative to
1013 historical dieback events and thus a greater decrease in C stock. Increased warming through time
1014 increasingly counteracts any CO₂ fertilization effect. While the amplitude of post-UCE C stock
1015 recoveries remains large, net C stock values eventually decline (downward curvature, and
1016 widening of the red shaded area) due to more pronounced loss in C stocks (and greater
1017 ecosystem state change) from hotter UCEs and longer recovery periods. We conceptualize how
1018 oscillations between SOs and MOs could be amplified and the widening of the shaded areas
1019 represents increased variability in how unprecedented eCO₂ levels and temperatures will affect
1020 ecosystems in the future compared to historical.
1021 SO = structural overshoot, MO = mortality overshoot, EE = historically extreme drought-heat
1022 event, UCE = unprecedented climate extreme.

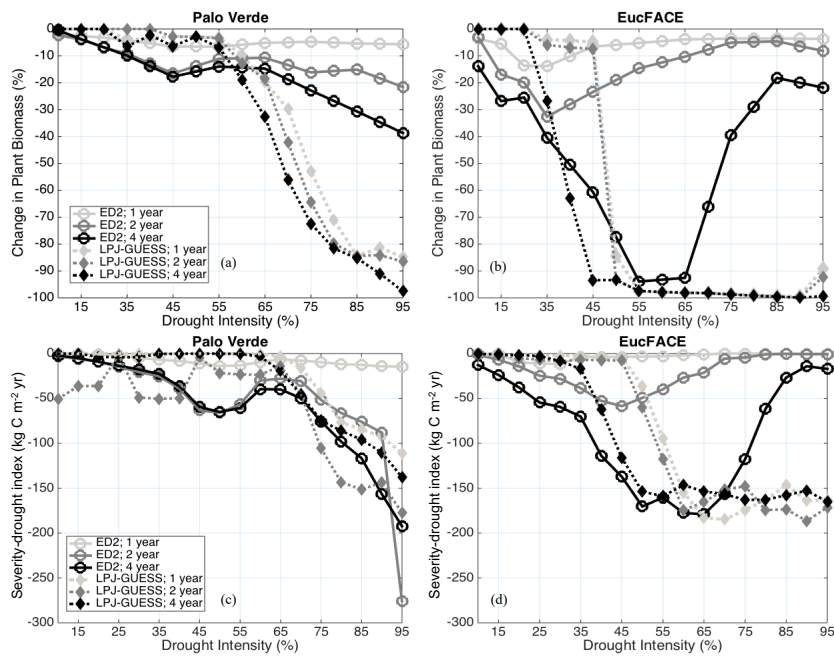
1023

Deleted: Integrated-C-change

Deleted: integrated-C-loss

Deleted: ;

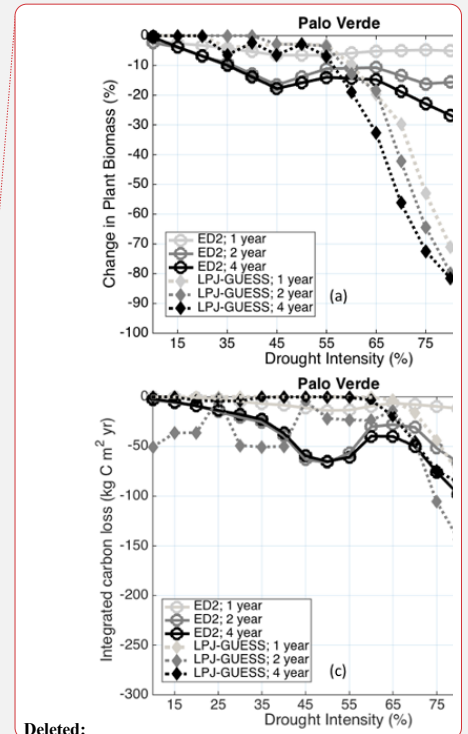
Deleted: w



1028

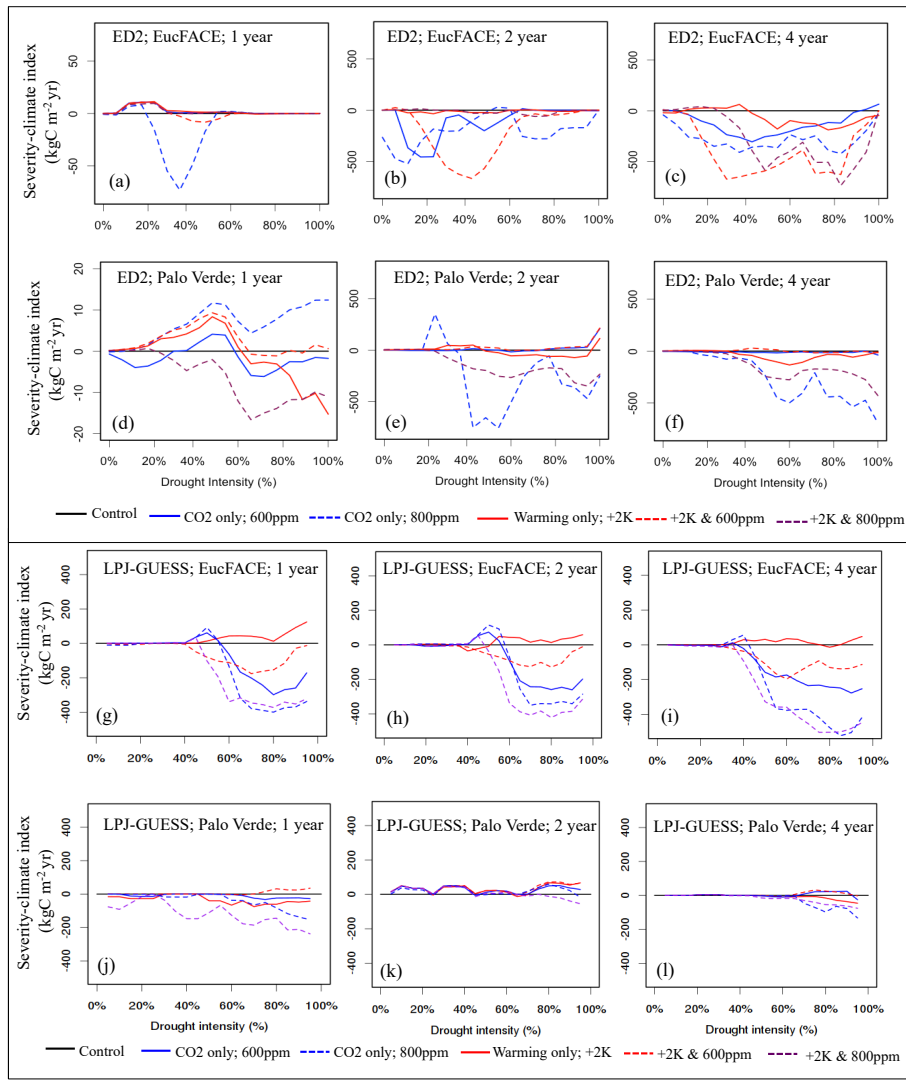
1029 **Figure 2** Modeled change in biomass (%) at the end of drought periods of different lengths (1, 2,
 1030 and 4-year droughts) and intensities (up to 95% precipitation removed) at (a) Palo Verde, and (b)
 1031 EucFACE, for the ED2 and LPJ-GUESS models. Modeled severity-drought index (C reduction
 1032 due to extreme drought integrated over time until biomass recovers to 50% of the non-drought
 1033 baseline biomass) at (c) Palo Verde and (d) EucFACE.

1034



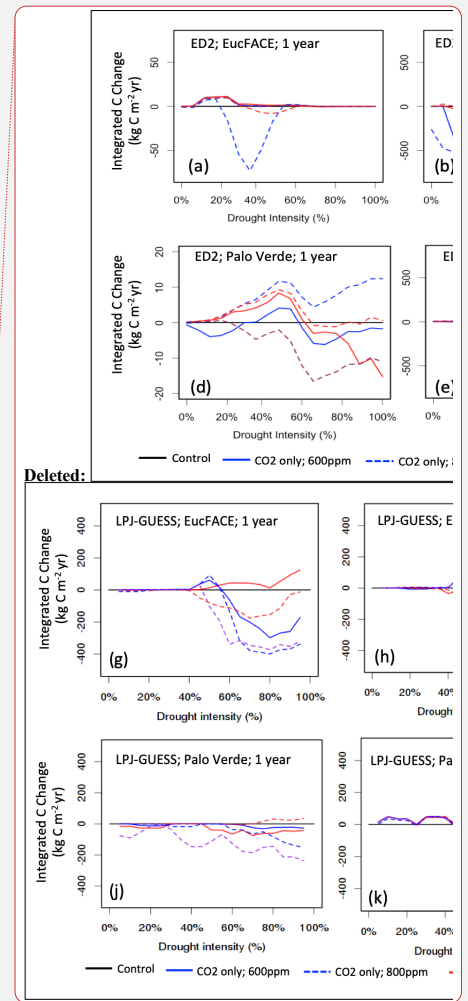
Deleted:

Deleted: integrated-C-loss



1037

1038 **Figure 3** Vegetation C response to interactions between drought intensity (0% to 100%
 1039 precipitation reduction), drought durations (1, 2, 4-year droughts), and idealized scenarios of
 1040 warming and eCO₂ compared to the control simulation, simulated by two VDMs; ED2 (a-f) and
 1041 LPJ-GUESS (g-l) at two sites (EucFACE and Palo Verde). The scenarios include a control



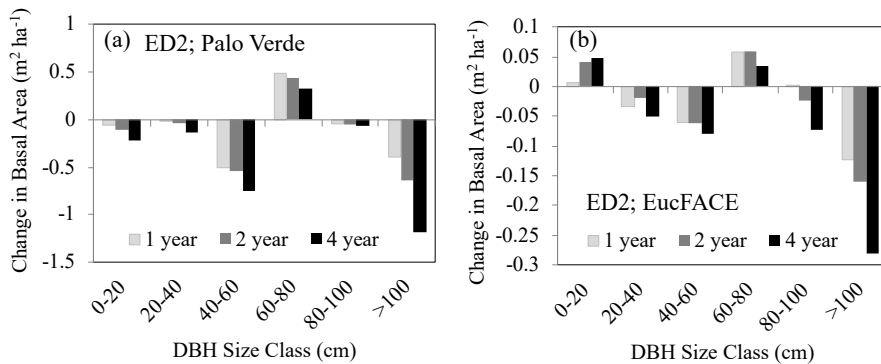
Deleted: reference

1045 (current temperature; 400 ppm atmospheric CO₂), two eCO₂ scenarios (600 ppm or 800 ppm),
 1046 elevated temperature (2 K above current), and a combination of eCO₂ (600 ppm or 800 ppm) and
 1047 higher temperature. Vegetation response is quantified as “severity-climate index” (in kg C m⁻²
 1048 yr; Eq. 4), which is defined as the difference between severity-drought index (i.e., carbon loss
 1049 due to only drought) and a given scenario of drought plus change in climatic drivers, relative to
 1050 the control (i.e., no climate change). Negative values for severity-climate index indicate that
 1051 warming and/or eCO₂ leads to stronger C losses and/or longer recovery, while positive values for
 1052 severity-climate index indicates a buffering effect.

Deleted: integrated-C-change
 Deleted: in
 Deleted: integrated-C-losses
 Deleted: between
 Deleted: and
 Deleted: integrated-C-change
 Deleted: integrated-C-change

1053

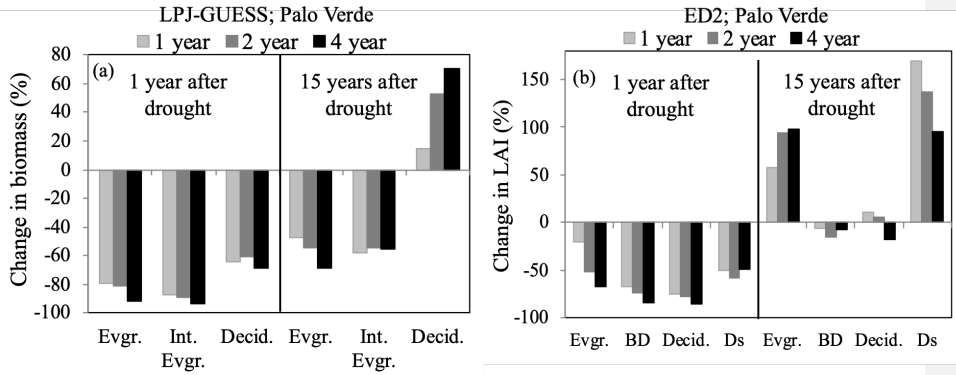
1054



1055

1056 **Figure 4** Change in basal area (m² ha⁻¹) immediately following either 1, 2, or 4 year droughts for
 1057 six increasing size class bins (DBH, cm) as predicted by the ED2 model for (a) the Palo Verde
 1058 site, with 90% precipitation removed, and (b) the EucFACE site with 50% precipitation
 1059 removed.

1067



1068

1069

1070 **Figure 5** Percent change in community composition, represented by plant functional type (PFT),
 1071 the year following three drought durations of UCEs (1, 2, and 4-year droughts and 90%
 1072 precipitation removed) as well as 15 years after droughts, for the tropical Palo Verde site by (a)
 1073 LPJ-GUESS reported in biomass change, and (b) ED2 reported in LAI change. Even though Ds
 1074 had the strongest recovery, it should be noted it was the least abundant PFT at this site. Evgr. =
 1075 evergreen, Int. Ever. = intermediate evergreen, Decid. = deciduous, BD = brevi-deciduous, Ds =
 1076 deciduous stem-succulent. EucFACE data not shown because only one PFT present (evergreen
 1077 tree).

1078 References:

1079

- 1080 Adams, H.D., Guardiola-Claramonte, M., Barron-Gafford, G.A., Villegas, J.C., Breshears, D.D.,
1081 Zou, C.B. et al.: Temperature sensitivity of drought-induced tree mortality portends
1082 increased regional die-off under global-change-type drought, *PNAS*, 106, 7063-7066, 2009.
- 1083 Adams, H.D., Barron-Gafford, G.A., Minor, R.L., Gardea, A.A., Bentley, L.P., Law, D.J. et al.:
1084 Temperature response surfaces for mortality risk of tree species with future drought,
1085 *Environ. Res. Lett.*, 12, 115014, 2017a.
- 1086 Adams, H.D., Zeppel, M.J.B., Anderegg, W.R.L., Hartmann, H., Landhäusser, S.M., Tissue, D.T.
1087 et al.: A multi-species synthesis of physiological mechanisms in drought-induced tree
1088 mortality, *Nature Ecol. & Evol.*, 1, 1285-1291, 2017b.
- 1089 Aguirre, BA, Hsieh, B, Watson, SJ, Wright, AJ.: The experimental manipulation of atmospheric
1090 drought: Teasing out the role of microclimate in biodiversity experiments, *J. Ecol.*, 109,
1091 1986– 1999, <https://doi.org/10.1111/1365-2745.13595>, 2021.
- 1092 Ahlström, A., Schurgers, G., Arneeth, A., and Smith, B.: Robustness and uncertainty in terrestrial
1093 ecosystem carbon response to CMIP5 climate change projections, *Environ. Res. Lett.*, 7,
1094 044008, 2012.
- 1095 Ainsworth, E.A., and Long, S.P.: What have we learned from 15 years of free-air CO₂
1096 enrichment (FACE)? A meta-analytic review of the responses of photosynthesis, canopy
1097 properties and plant production to rising CO₂, *New Phytol.*, 165, 351-372, 2005.
- 1098 Allen, C.D., Breshears, D.D., and McDowell, N.G.: On underestimation of global vulnerability to
1099 tree mortality and forest die-off from hotter drought in the Anthropocene, *Ecosphere*, 6,
1100 art129, 2015.
- 1101 Allen, K., Dupuy, J.M., Gei, M.G., Hulshof, C.M., Medvigy, D., Pizano, C. et al.: Will seasonally
1102 dry tropical forests be sensitive or resistant to future changes in 558 rainfall regimes?
1103 *Environ. Res. Lett.*, 12, 023001, 2017.
- 1104 Amiro, B.D., Barr, A.G., Barr, J.G., Black, T.A., Bracho, R., Brown, M. et al.: Ecosystem carbon
1105 dioxide fluxes after disturbance in forests of North America, *J. Geophys. Res.*
1106 *Biogeosciences*, 115, 2010.
- 1107 Anderegg, W.R.L., Hicke, J.A., Fisher, R.A., Allen, C.D., Aukema, J., Bentz, B. et al.: Tree
1108 mortality from drought, insects, and their interactions in a changing climate, *New Phytol.*,
1109 208, 674-683, 2015.
- 1110 Anderegg, W.R.L., Klein, T., Bartlett, M., Sack, L., Pellegrini, A.F.A., Choat, B. et al.: Meta-
1111 analysis reveals that hydraulic traits explain cross-species patterns of drought-induced tree
1112 mortality across the globe, *PNAS*, 113, 5024-5029, 2016a.
- 1113 Anderegg, W.R.L., Martinez-Vilalta, J., Cailleret, M., Camarero, J.J., Ewers, B.E., Galbraith, D.
1114 et al.: When a Tree Dies in the Forest: Scaling Climate-Driven Tree Mortality to Ecosystem
1115 Water and Carbon Fluxes, *Ecosystems*, 19, 1133-1147, 2016b.
- 1116 Anderegg, W.R.L., Konings, A.G., Trugman, A.T., Yu, K., Bowling, D.R., Gabbitas, R. et al.:
1117 Hydraulic diversity of forests regulates ecosystem resilience during drought, *Nature*, 561,
1118 538-541, 2018.
- 1119 Anderegg, W.R.L. and Venturas, M.D.: Plant hydraulics play a critical role in Earth system
1120 fluxes, *New Phytol.*, 226, 1535-1538, <https://doi.org/10.1111/nph.16548>, 2020.
- 1121 Asner, G.P., Brodrick, P.G., Anderson, C.B., Vaughn, N., Knapp, D.E., and Martin, R.E.:
1122 Progressive forest canopy water loss during the 2012–2015 California drought. *PNAS*, 113,
1123 E249-E255, 2016.

1124 Arora, V.K., Katavouta, A., Williams, R.G., Jones, C.D., Brovkin, V., Friedlingstein, P., et al.:
1125 Carbon-concentration and carbon-climate feedbacks in CMIP6 models and their
1126 comparison to CMIP5 models, *Biogeosciences*, 17, 4173–4222, 2020.

1127 Bai, Y., Wu, J., Xing, Q., Pan, Q., Huang, J., Yang, D. et al.: PRIMARY PRODUCTION AND
1128 RAIN USE EFFICIENCY ACROSS A PRECIPITATION GRADIENT ON THE
1129 MONGOLIA PLATEAU, *Ecology*, 89, 2140-2153, 2008.

1130 Beier, C., Beierkuhnlein, C., Wohlgemuth, T., Penuelas, J., Emmett, B., Körner, C. et al.:
1131 Precipitation manipulation experiments – challenges and recommendations for the future,
1132 *Ecol. Lett.*, 15, 899-911, 2012.

1133 Bennett, A.C., McDowell, N.G., Allen, C.D., and Anderson-Teixeira, K.J.: Larger trees suffer
1134 most during drought in forests worldwide, *Nature Plants*, 1, 15139, 2015.

1135 Biederman, J.A., Meixner, T., Harpold, A.A., Reed, D.E., Gutmann, E.D., Gaun, J.A. et al.:
1136 Riparian zones attenuate nitrogen loss following bark beetle-induced lodgepole pine
1137 mortality, *J. Geophys. Res. Biogeosciences*, 121, 933-948, 2016.

1138 Biederman, J.A., Somor, A.J., Harpold, A.A., Gutmann, E.D., Breshears, D.D., Troch, P.A. et al.:
1139 Recent tree die-off has little effect on streamflow in contrast to expected increases from
1140 historical studies, *Water Resources Res.*, 51, 9775-9789, 2015.

1141 Blyth, E.M., Arora, V.K., Clark, D.B. et al.: Advances in Land Surface Modelling, *Curr. Clim.*
1142 *Change Rep.*, 7, 45–71, <https://doi.org/10.1007/s40641-021-00171-5>, 2021.

1143 Borchert, R., Rivera, G., and Hagnauer, W.: Modification of Vegetative Phenology in a Tropical
1144 Semi-deciduous Forest by Abnormal Drought and Rain, *Biotropica*, 34, 27-39, 2002.

1145 Bonan, G.: *Vegetation Demography*, in: *Climate Change and Terrestrial Ecosystem Modeling*,
1146 Cambridge: Cambridge University Press, 344-364, doi:10.1017/9781107339217.020, 2019.

1147 Bonan, G. B., Patton, E. G., Finnigan, J. J., Baldocchi, D. D., and Harman, I. N.: Moving beyond
1148 the incorrect but useful paradigm: reevaluating big-leaf and multilayer plant canopies to
1149 model biosphere-atmosphere fluxes – a review, *Agr. Forest Meteorol.*, 306,
1150 108435, <https://doi.org/10.1016/j.agrformet.2021.108435>, 2021.

1151 Brando, P.M., Paolucci, L., Ummenhofer, C.C., Ordway, E.M., Hartmann, H., Cattau, M.E.,
1152 Rattis, L., Medjibe, V., Coe, M.T., Balch, J.: Droughts, Wildfires, and Forest Carbon
1153 Cycling: A Pantropical Synthesis, *Annual Review of Earth and Planetary Sciences*, 47, 555-
1154 581, 2019.

1155 Breshears, D.D., Myers, O.B., Meyer, C.W., Barnes, F.J., Zou, C.B., Allen, C.D. et al.: Tree die-
1156 off in response to global change-type drought: mortality insights from a decade of plant
1157 water potential measurements, *Front. Ecol. Environ.*, 7, 185-189, 2009.

1158 Brodribb, T.J., Bowman, D.J.M.S., Nichols, S., Delzon, S. and Burlett, R.: Xylem function and
1159 growth rate interact to determine recovery rates after exposure to extreme water deficit, *New*
1160 *Phytol.*, 188, 533-542, 2010.

1161 Bugmann, H., and Seidl, R.: The evolution, complexity and diversity of models of long-term
1162 forest dynamics. *J. of Ecol.*, 110, 2288– 2307, <https://doi.org/10.1111/1365-2745.13989>,
1163 2022.

1164 Carreño-Rocabado, G., Peña-Claros, M., Bongers, F., Alarcón, A., Licona, J.-C., and Poorter, L.:
1165 Effects of disturbance intensity on species and functional diversity in a tropical forest, *J.*
1166 *Ecology*, 100, 1453-1463, 2012.

1167 Chapman, T.B., Veblen, T.T., and Schoennagel, T.: Spatiotemporal patterns of mountain pine
1168 beetle activity in the southern Rocky Mountains, *Ecology*, 93, 2175-2185, 2012.

1169 Chiang, F., Mazdiyasi, O., and AghaKouchak, A.: Evidence of anthropogenic impacts on global
1170 drought frequency, duration, and intensity, *Nat Commun.*, 12, 2754,
1171 <https://doi.org/10.1038/s41467-021-22314-w>, 2021.

1172 Choat, B., Brodribb, T.J., Brodersen, C.R., Duursma, R.A., López, R., and Medlyn, B.E.: Triggers
1173 of tree mortality under drought, *Nature*, 558, 531-539, 2018.

1174 Choat, B., Jansen, S., Brodribb, T.J., Cochard, H., Delzon, S., Bhaskar, R. et al.: Global
1175 convergence in the vulnerability of forests to drought, *Nature*, 491, 752-755, 2012.

1176 Christoffersen, B.O., Gloor, M., Fauset, S., Fyllas, N.M., Galbraith, D.R., Baker, T.R. et al.:
1177 Linking hydraulic traits to tropical forest function in a size-structured and trait-driven model
1178 (TFS v.1-Hydro), *Geosci. Model Dev. Discuss.*, 2016, 1-60, 2016.

1179 Ciais, P., Reichstein, M., Viovy, N., Granier, A., Ogée, J., Allard, V. et al.: Europe-wide
1180 reduction in primary productivity caused by the heat and drought in 2003, *Nature*, 437, 529,
1181 2005.

1182 Clark, K.L., Skowronski, N., and Hom, J.: Invasive insects impact forest carbon dynamics, *Glob.
1183 Change Biol.*, 16, 88-101, 2010.

1184 Coley, P., Massa, M., Lovelock, C., Winter, K.: Effects of elevated CO₂ on foliar chemistry of
1185 saplings of nine species of tropical tree, *Oecologia*, 2002.

1186 Creeden, E.P., Hicke, J.A., and Buotte, P.C.: Climate, weather, and recent mountain pine beetle
1187 outbreaks in the western United States, *Forest Ecol. Manag.*, 312, 239-251, 2014.

1188 D'Amato, A.W., Bradford, J.B., Fraver, S. and Palik, B.J.: Effects of thinning on drought
1189 vulnerability and climate response in north temperate forest ecosystems, *Eco. Applications*,
1190 23, 1735-1742, 2013.

1191 da Costa, A.C.L., Galbraith, D., Almeida, S., Portela, B.T.T., da Costa, M., de Athaydes Silva
1192 Junior, J. et al., Effect of 7 yr of experimental drought on vegetation dynamics and biomass
1193 storage of an eastern Amazonian rainforest, *New Phytol.*, 187, 579-591, 2010.

1194 De Kauwe, M.G., Medlyn, B.E., Zaehle, S., Walker, A.P., Dietze, M.C., Wang, Y.-P. et al.:
1195 Where does the carbon go? A model-data intercomparison of vegetation carbon allocation
1196 and turnover processes at two temperate forest free-air CO₂ enrichment sites, *New Phytol*,
1197 203, 883-899, 2014.

1198 Dietze, M.C., and Matthes, J.H.: A general ecophysiological framework for modelling the impact
1199 of pests and pathogens on forest ecosystems, *Ecol. Lett.*, 17, 1418-1426, 2014.

1200 Döscher, R., Acosta, M., et al.: The EC-Earth3 Earth System Model for the Climate Model
1201 Intercomparison Project 6, *Geosci. Model Dev. Discuss.* [preprint],
1202 <https://doi.org/10.5194/gmd-2020-446>, in revision, 2022.

1203 Dreesen, F.E., De Boeck, H.J., Janssens, I.A., and Nijs, I.: Do successive climate extremes
1204 weaken the resistance of plant communities? An experimental study using plant
1205 assemblages, *Biogeosciences*, 11, 109-121, 2014.

1206 Eamus, D., Boulain, N., Cleverly, J., and Breshears, D.D.: Global change-type drought-induced
1207 tree mortality: vapor pressure deficit is more important than temperature per se in causing
1208 decline in tree health, *Ecol. Evol.*, 3, 2711-2729, 2013.

1209 Eller, C.B., Rowland, L., Mencuccini, M., Rosas, T., Williams, K., Harper, A. et al.: Stomatal
1210 optimization based on xylem hydraulics (SOX) improves land surface model simulation of
1211 vegetation responses to climate, *New Phytol*, 226, 1622-
1212 1637, <https://doi.org/10.1111/nph.16419>, 2020.

Deleted: Ciais, P., Sabine, C., Bala, G., Bopp, L., Brovkin, V., Canadell, J., et al.: Carbon and other biogeochemical cycles. In: *Climate Change 2013: The Physical Science Basis. Contribution of Working Group I to the Fifth Assessment Report of the Intergovernmental Panel on Climate Change* (eds. Stocker, T.F., Qin, D., Plattner, G.-K., Tignor, M., Allen, S.K., Boschung, J., et al.), Cambridge University Press, Cambridge, United Kingdom and New York, NY, USA, pp. 465-570, 2013. ¶

Deleted: Duursma, R.A., Gimeno, T.E., Boer, M.M., Crous, K.Y., Tjoelker, M.G. and Ellsworth, D.S.: Canopy leaf area of a mature evergreen *Eucalyptus* woodland does not respond to elevated atmospheric [CO₂] but tracks water availability, *Glob. Change Biol.*, 22, 1666-1676, <https://doi.org/10.1111/gcb.13151>, 2016. ¶

1228 Ellsworth, David S., Anderson, Ian C., Crous, Kristine Y., Cooke, J., Drake, John E., Gherlenda,
1229 Andrew N. et al.: Elevated CO₂ does not increase eucalypt forest productivity on a low-
1230 phosphorus soil, *Nature Climate Change*, 7, 279, 2017.

1231 ENQUIST, B.J., and ENQUIST, C.A.F.: Long-term change within a Neotropical forest: assessing
1232 differential functional and floristic responses to disturbance and drought, *Glob. Change*
1233 *Biol.*, 17, 1408-1424, 2011.

1234 Esquivel-Muelbert, A., Baker, T.R., Dexter, K.G., Lewis, S.L., Brienen, R.J.W., Feldpausch, T.R.
1235 et al.: Compositional response of Amazon forests to climate change, *Glob. Change Biol.*, 25,
1236 39-56, 2019.

1237 Eziz, A., Yan, Z., Tian, D., Han, W., Tang, Z., and Fang, J.: Drought effect on plant biomass
1238 allocation: A meta-analysis, *Ecol. Evol.*, 7, 11002-11010, 2017.

1239 Fang, Y., Leung, L. R., Knox, R., Koven, C., and Bond-Lamberty, B.: Impact of the numerical
1240 solution approach of a plant hydrodynamic model (v0.1) on vegetation dynamics, *Geosci.*
1241 *Model Dev.*, 15, 6385–6398, <https://doi.org/10.5194/gmd-15-6385-2022>, 2022.

1242 Feldpausch, T.R., Phillips, O.L., Brienen, R.J.W., Gloor, E., Lloyd, J., Lopez-Gonzalez, G. et al.:
1243 Amazon forest response to repeated droughts, *Global Biogeochemical Cycles*, 30, 964-982,
1244 2016.

1245 Fisher, R.A., Muszala, S., Versteinstein, M., Lawrence, P., Xu, C., McDowell, N.G. et al.: Taking
1246 off the training wheels: the properties of a dynamic vegetation model without climate
1247 envelopes, *CLM4.5(ED)*, *Geosci. Model Dev.*, 8, 3593-3619, 2015.

1248 Fisher, R.A., Koven, C.D., Anderegg, W.R.L., Christoffersen, B.O., Dietze, M.C., Farrior, C.E. et
1249 al.: Vegetation demographics in Earth System Models: A review of progress and priorities,
1250 *Glob. Change Biol.*, 24, 35-54, 2018.

1251 Fisher, R. A., and Koven, C. D.: Perspectives on the future of land surface models and the
1252 challenges of representing complex terrestrial systems, *JAMES*, 12,
1253 e2018MS001453, <https://doi.org/10.1029/2018MS001453>, 2020.

1254 Fleischer, K., Rammig, A., De Kauwe, M.G., Walker, A.P., Domingues, T.F., Fuchslueger, L. et
1255 al.: Amazon forest response to CO₂ fertilization dependent on plant phosphorus acquisition,
1256 *Nature Geoscience*, 12, 736-741, 2019.

1257 Frank, D., Reichstein, M., Bahn, M., Thonicke, K., Frank, D., Mahecha, M.D. et al.: Effects of
1258 climate extremes on the terrestrial carbon cycle: concepts, processes and potential future
1259 impacts, *Glob. Change Biol.*, 21, 2861-2880, 2015.

1260 Franklin, O., McMurtrie, R.E., Iversen, C.M., Crous, K.Y., Finzi, A.C., Tissue, D.T., Ellsworth,
1261 D.S., Oren, R. Norby, R.J.: Forest fine-root production and nitrogen use under elevated
1262 CO₂: contrasting responses in evergreen and deciduous trees explained by a common
1263 principle, *Glob. Change Biol.*, 15, 132-144, 2009.

1264 Franklin, O., Johansson, J., Dewar, R.C., Dieckmann, U., McMurtrie, R.E., Brännström, Å.,
1265 Dybzinski, R.: Modeling carbon allocation in trees: a search for principles, *Tree Physiology*,
1266 32, 648–666, <https://doi.org/10.1093/treephys/tpr138>, 2012.

1267 Franklin, O., Harrison, S.P., Dewar, R. et al.: Organizing principles for vegetation dynamics. *Nat.*
1268 *Plants*, 6, 444–453, <https://doi.org/10.1038/s41477-020-0655-x>, 2020.

1269 Friend, A.D., Lucht, W., Rademacher, T.T., Keribin, R., Betts, R., Cadule, P. et al.: Carbon
1270 residence time dominates uncertainty in terrestrial vegetation responses to future climate
1271 and atmospheric CO₂, *PNAS*, 111, 3280-3285, 2014.

1272 Gerten, D., LUO, Y., Le MAIRE, G., PARTON, W.J., KEOUGH, C., WENG, E. et al.: Modelled
1273 effects of precipitation on ecosystem carbon and water dynamics in different climatic zones,
1274 *Glob. Change Biol.*, 14, 2365-2379, 2008.

1275 Goulden, M.L., and Bales, R.C.: California forest die-off linked to multi-year deep soil drying in
1276 2012–2015 drought, *Nature Geoscience*, 12, 632-637, 2019.

1277 Gray, S.B., Dermody, O., Klein, S.P., Locke, A.M., McGrath, J.M., Paul, R.E. et al.: Intensifying
1278 drought eliminates the expected benefits of elevated carbon dioxide for soybean, *Nature*
1279 *Plants*, 2, 16132, 2016.

1280 Greenwood, S., Ruiz-Benito, P., Martínez-Vilalta, J., Lloret, F., Kitzberger, T., Allen, C.D. et al.:
1281 Tree mortality across biomes is promoted by drought intensity, lower wood density and
1282 higher specific leaf area, *Ecol. Lett.*, 20, 539-553, 2017.

1283 Griffin, D., and Anchukaitis, K.J.: How unusual is the 2012–2014 California drought? *Geophys.*
1284 *Res. Lett.*, 41, 9017-9023, 2014.

1285 Hanbury-Brown, A.R., Powell, T.L., Muller-Landau, H.C., Wright, S.J. and Kueppers, L.M.:
1286 Simulating environmentally-sensitive tree recruitment in vegetation demographic models,
1287 *New Phytol.*, 235, 78-93, <https://doi.org/10.1111/nph.18059>, 2022.

1288 Harrison, S.P., Cramer, W., Franklin, O., Prentice, I.C., Wang, H., Brännström, Å., et al.: Eco-
1289 evolutionary optimality as a means to improve vegetation and land-surface models, *New*
1290 *Phytol.*, 231, 2125-2141, <https://doi.org/10.1111/nph.17558>, 2021.

1291 Hickler, T., Smith, B., Sykes, M.T., Davis, M.B., Sugita, S., and Walker, K.: USING A
1292 GENERALIZED VEGETATION MODEL TO SIMULATE VEGETATION DYNAMICS
1293 IN NORTHEASTERN USA, *Ecology*, 85, 519-530, 2004.

1294 Holm, J. A., Knox, R. G., Zhu, Q., Fisher, R. A., Koven, C. D., Nogueira Lima, A. J., et al.: The
1295 central Amazon biomass sink under current and future atmospheric CO₂: Predictions from
1296 big-leaf and demographic vegetation models, *J. Geophys. Res. Biogeosciences*, 125,
1297 e2019JG005500. <https://doi.org/10.1029/2019JG005500>, 2020.

1298 Hovenden, M.J., Newton, P.C.D., and Wills, K.E.: Seasonal not annual rainfall determines
1299 grassland biomass response to carbon dioxide, *Nature*, 511, 583, 2014.

1300 Hubbard, R.M., Rhoades, C.C., Elder, K., and Negrón, J.: Changes in transpiration and foliage
1301 growth in lodgepole pine trees following mountain pine beetle attack and mechanical
1302 girdling, *Forest Ecol. Manag.*, 289, 312-317, 2013.

1303 IPCC: Managing the Risks of Extreme Events and Disasters to Advance Climate Change
1304 Adaptation. A Special Report of Working Groups I and II of the Intergovernmental Panel on
1305 Climate Change. (ed. Field, C.B., V. Barros, T.F. Stocker, D. Qin, D.J. Dokken, K.L. Ebi,
1306 M.D. Mastrandrea, K.J. Mach, G.-K. Plattner, S.K. Allen, M. Tignor, and P.M. Midgley)
1307 Cambridge, UK, and New York, NY, USA, p. 582 pp, 2012.

1308 IPCC: Climate Change 2021: The Physical Science Basis. Contribution of Working Group I to the
1309 Sixth Assessment Report of the Intergovernmental Panel on Climate Change [Masson-
1310 Delmotte, V., P. Zhai, A. Pirani, S.L. Connors, C. Péan, S. Berger, N. Caud, Y. Chen, L.
1311 Goldfarb, M.I. Gomis, M. Huang, K. Leitzell, E. Lonnoy, J.B.R. Matthews, T.K. Maycock,
1312 T. Waterfield, O. Yelekçi, R. Yu, and B. Zhou (eds.)]. Cambridge University Press, 2021.

1313 Jiang, M., Medlyn, B.E., Drake, J.E., Duursma, R.A., Anderson, I.C., Barton, C.V.M., Boer,
1314 M.B., Carrillo, Y., Castañeda-Gómez, L., Collins, L., et al.: The fate of carbon in a mature
1315 forest under carbon dioxide enrichment, *Nature*, 580, 227-231,
1316 <https://doi.org/10.1038/s41586-020-2128-9>, 2020.

1317 Joslin, J.D., Wolfe, M.H., and Hanson, P.J.: Effects of altered water regimes on forest root
1318 systems, *New Phytol.*, 147, 117-129, 2000.

1319 Jump, A.S., Ruiz-Benito, P., Greenwood, S., Allen, C.D., Kitzberger, T., Fensham, R. et al.:
1320 Structural overshoot of tree growth with climate variability and the global spectrum of
1321 drought-induced forest dieback, *Glob. Change Biol.*, 23, 3742-3757, 2017.

1322 Kalacska, M.E.R., Sánchez-Azofeifa, G.A., Calvo-Alvarado, J.C., Rivard, B. and Quesada, M.:
1323 Effects of Season and Successional Stage on Leaf Area Index and Spectral Vegetation
1324 Indices in Three Mesoamerican Tropical Dry Forests, *Biotropica*, 37, 486-
1325 496, <https://doi.org/10.1111/j.1744-7429.2005.00067.x>, 2005.

1326 Kannenberg, S.A., Schwalm, C.R. and Anderegg, W.R.L.: Ghosts of the past: how drought legacy
1327 effects shape forest functioning and carbon cycling, *Ecol. Lett.*, 23: 891-901,
1328 <https://doi.org/10.1111/ele.13485>, 2020.

1329 Kattge, J., DÍAZ, S., LAVOREL, S., PRENTICE, I.C., LEADLEY, P., BÖNISCH, G. et al.: TRY
1330 – a global database of plant traits, *Global Change Biol.*, 17, 2905-2935, 2011.

1331 Kayler, Z.E., De Boeck, H.J., Fatichi, S., Grünzweig, J.M., Merbold, L., Beier, C. et al.:
1332 Experiments to confront the environmental extremes of climate change, *Front. Ecol.*
1333 *Environ.*, 13, 219-225, 2015.

1334 Keenan, T.F., Hollinger, D.Y., Bohrer, G., Dragoni, D., Munger, J.W., Schmid, H.P. et al.:
1335 Increase in forest water-use efficiency as atmospheric carbon dioxide concentrations rise,
1336 *Nature*, 499, 324-327, 2013.

1337 Kennedy, D., Swenson, S., Oleson, K. W., Lawrence, D. M., Fisher, R., Lola da Costa, A. C., and
1338 Gentine, P.: Implementing plant hydraulics in the Community Land Model, version 5,
1339 *JAMES*, 11, 485– 513, <https://doi.org/10.1029/2018MS001500>, 2019.

1340 Li, L., Yang, Z.-L., Matheny, A. M., Zheng, H., Swenson, S. C., Lawrence, D. M., et
1341 al.: Representation of plant hydraulics in the Noah-MP land surface model: Model
1342 development and multiscale evaluation, *JAMES*, 13,
1343 e2020MS002214, <https://doi.org/10.1029/2020MS002214>, 2021.

1344 Li, Q., Lu, X., Wang, Y., Huang, X., Cox, P. M., and Luo, Y.: Leaf area index identified as a
1345 major source of variability in modeled CO₂ fertilization, *Biogeosciences*, 15, 6909–6925,
1346 <https://doi.org/10.5194/bg-15-6909-2018>, 2018.

1347 Liu, Y., Parolari, A.J., Kumar, M., Huang, C.-W., Katul, G.G., and Porporato, A.: Increasing
1348 atmospheric humidity and CO₂ concentration alleviate forest mortality risk, *PNAS*, 114,
1349 9918-9923, 2017.

1350 Lloret, F., Escudero, A., Iriondo, J.M., Martínez-Vilalta, J., and Valladares, F.: Extreme climatic
1351 events and vegetation: the role of stabilizing processes, *Glob. Change Biol.*, 18, 797-805,
1352 2012.

1353 Luo, Y., Gerten, D., Le Maire, G., Parton, W.J., Weng, E., Zhou, X. et al.: Modeled interactive
1354 effects of precipitation, temperature, and [CO₂] on ecosystem carbon and water dynamics in
1355 different climatic zones, *Glob. Change Biol.*, 14, 1986-1999, 2008.

1356 Luo, Y.Q., Randerson, J.T., Abramowitz, G., Bacour, C., Blyth, E., Carvalhais, N. et al.: A
1357 framework for benchmarking land models, *Biogeosciences*, 9, 3857-3874, 2012.

1358 Luo, Y., Jiang, L., Niu, S., Zhou, X.: Nonlinear responses of land ecosystems to variation in
1359 precipitation, *New Phytol.*, 214, 5–7, 2017.

1360 Ma, W., Zhai, L., Pivovarov, A., Shuman, J., Buotte, P., Ding, J., Christoffersen, B., Knox, R.,
1361 Moritz, M., Fisher, R. A., Koven, C. D., Kueppers, L., and Xu, C.: Assessing climate

1362 change impacts on live fuel moisture and wildfire risk using a hydrodynamic vegetation
 1363 model, *Biogeosciences*, 18, 4005–4020, <https://doi.org/10.5194/bg-18-4005-2021>, 2021.
 1364 MacGillivray, C.W., Grime, J.P., and The Integrated Screening Programme, T.: Testing
 1365 Predictions of the Resistance and Resilience of Vegetation Subjected to Extreme Events,
 1366 *Funct. Ecol.*, 9, 640-649, 1995.
 1367 Markewitz, D., Devine, S., Davidson, E.A., Brando, P., and Nepstad, D.C.: Soil moisture
 1368 depletion under simulated drought in the Amazon: impacts on deep root uptake, *New*
 1369 *Phytol.*, 187, 592-607, 2010.
 1370 Matusick, G., Ruthrof, K.X., Brouwers, N.C., Dell, B., and Hardy, G.S.J.: Sudden forest canopy
 1371 collapse corresponding with extreme drought and heat in a mediterranean-type eucalypt
 1372 forest in southwestern Australia, *European J. Forest Res.*, 132, 497-510, 2013.
 1373 Matusick, G., Ruthrof, K.X., Fontaine, J.B., and Hardy, G.E.S.J.: Eucalyptus forest shows low
 1374 structural resistance and resilience to climate change-type drought, *J. Vegetation Science*,
 1375 27, 493-503, 2016.
 1376 McCarthy, M.C., and Enquist, B.J.: Consistency between an allometric approach and optimal
 1377 partitioning theory in global patterns of plant biomass allocation, *Funct. Ecol.*, 21, 713-720,
 1378 2007.
 1379 McDowell, N., Pockman, W.T., Allen, C.D., Breshears, D.D., Cobb, N., Kolb, T. et al.:
 1380 Mechanisms of plant survival and mortality during drought: why do some plants survive
 1381 while others succumb to drought? *New Phytol.*, 178, 719-739, 2008.
 1382 McDowell, N.G., Adams, H.D., Bailey, J.D., Hess, M., and Kolb, T.E.: Homeostatic Maintenance
 1383 Of Ponderosa Pine Gas Exchange In Response To Stand Density Changes, *Ecological*
 1384 *Applications*, 16, 1164-1182, 2006.
 1385 McDowell, N.G., and Allen, C.D.: Darcy's law predicts widespread forest mortality under climate
 1386 warming, *Nature Climate Change*, 5, 669-672, 2015.
 1387 McDowell, N.G., Beerling, D.J., Breshears, D.D., Fisher, R.A., Raffa, K.F., and Stitt, M.: The
 1388 interdependence of mechanisms underlying climate-driven vegetation mortality, *Trends in*
 1389 *Ecol. & Evolution*, 26, 523-532, 2011.
 1390 McDowell, N.G., Fisher, R.A., Xu, C., Domec, J.C., Hölttä, T., Mackay, D.S. et al.: Evaluating
 1391 theories of drought-induced vegetation mortality using a multimodel–experiment
 1392 framework, *New Phytol.*, 200, 304-321, 2013.
 1393 Medlyn, B.E., De Kauwe, M.G., Zaehle, S., Walker, A.P., Duursma, R.A., Luus, K., Mishurov,
 1394 M., Pak, B., Smith, B., Wang, Y.-P., Yang, X., Crous, K.Y., Drake, J.E., Gimeno, T.E.,
 1395 Macdonald, C.A., Norby, R.J., Power, S.A., Tjoelker, M.G. and Ellsworth, D.S.: Using
 1396 models to guide field experiments: a priori predictions for the CO₂ response of a nutrient-
 1397 and water-limited native Eucalypt woodland, *Glob. Change Biol.*, 22, 2834-2851, 2016.
 1398 Medvigy, D., Wang, G., Zhu, Q., Riley, W.J., Trierweiler, A.M., Waring, B., Xu, X. and Powers,
 1399 J.S.: Observed variation in soil properties can drive large variation in modelled forest
 1400 functioning and composition during tropical forest secondary succession, *New Phytol.*, 223,
 1401 1820-1833, <https://doi.org/10.1111/nph.15848>, 2019.
 1402 Medvigy, D., Clark, K.L., Skowronski, N.S., and Schäfer, K.V.R.: Simulated impacts of insect
 1403 defoliation on forest carbon dynamics, *Environ. Res. Lett.*, 7, 045703, 2012.
 1404 Medvigy, D. and Moorcroft, P.R.: Predicting ecosystem dynamics at regional scales: an
 1405 evaluation of a terrestrial biosphere model for the forests of northeastern North America,
 1406 *Philosophical Transactions of the Royal Society B: Biological Sciences*, 367, 222-235,
 1407 2012.

1408 Medvigy, D., Wofsy, S., Munger, J., Hollinger, D. and Moorcroft, P.: Mechanistic scaling of
1409 ecosystem function and dynamics in space and time: Ecosystem Demography model version
1410 2, *J. Geophys. Res. Biogeosciences*, 114, 2009.

1411 Mencuccini, M., Manzoni, S., and Christoffersen, B.: Modelling water fluxes in plants: from
1412 tissues to biosphere, *New Phytol.*, 222, 1207-1222, <https://doi.org/10.1111/nph.15681>, 2019.

1413 Meir, P., Wood, T.E., Galbraith, D.R., Brando, P.M., Da Costa, A.C.L., Rowland, L. et al.:
1414 Threshold Responses to Soil Moisture Deficit by Trees and Soil in Tropical Rain Forests:
1415 Insights from Field Experiments, *BioScience*, 65, 882-892, 2015.

1416 Montané, F., Fox, A.M., Arellano, A.F., MacBean, N., Alexander, M.R., Dye, A. et al.:
1417 Evaluating the effect of alternative carbon allocation schemes in a land surface model
1418 (CLM4.5) on carbon fluxes, pools, and turnover in temperate forests, *Geosci. Model Dev.*,
1419 10, 3499-3517, 2017.

1420 Muldavin, E.H., Moore, D.I., Collins, S.L., Wetherill, K.R., and Lightfoot, D.C.: Aboveground
1421 net primary production dynamics in a northern Chihuahuan Desert ecosystem, *Oecologia*,
1422 155, 123-132, 2008.

1423 Myers, J.A., and Kitajima, K.: Carbohydrate storage enhances seedling shade and stress tolerance
1424 in a neotropical forest, *J. Ecology*, 95, 383-395, 2007.

1425 Niklas, K. J.: The scaling of plant height: A comparison among major plant clades and anatomical
1426 grades, *Annals of Botany*, 72, 165-172, <https://doi.org/10.1006/anbo.1993.1095>, 1993.

1427 Norby, R.J., DeLucia, E.H., Gielen, B., Calfapietra, C., Giardina, C.P., King, J.S. et al.: Forest
1428 response to elevated CO₂ is conserved across a broad range of productivity, *PNAS*, 102,
1429 18052-18056, 2005.

1430 O'Brien, M.J., Leuzinger, S., Philipson, C.D., Tay, J., and Hector, A.: Drought survival of
1431 tropical tree seedlings enhanced by non-structural carbohydrate levels, *Nature Climate
1432 Change*, 4, 710, 2014.

1433 Obermeier, W.A., Lehnert, L.W., Kammann, C.I., Müller, C., Grünhage, L., Luterbacher, J. et al.:
1434 Reduced CO₂ fertilization effect in temperate C₃ grasslands under more extreme weather
1435 conditions, *Nature Climate Change*, 7, 137, 2016.

1436 Palace, M., Keller, M., and Silva, H.: NECROMASS PRODUCTION: STUDIES IN
1437 UNDISTURBED AND LOGGED AMAZON FORESTS, *Ecological Applications*, 18, 873-
1438 884, 2008.

1439 Petit, G., Anfodillo, T., Mencuccini, M.: Tapering of xylem conduits and hydraulic limitations in
1440 sycamore (*Acer pseudoplatanus*) trees, *New Phytol.*, 177, 653-
1441 664. <https://doi.org/10.1111/j.1469-8137.2007.02291.x>, 2008.

1442 Phillips, O.L., Aragão, L.E.O.C., Lewis, S.L., Fisher, J.B., Lloyd, J., López-González, G. et al.:
1443 Drought Sensitivity of the Amazon Rainforest, *Science*, 323, 1344-1347, 2009.

1444 Phillips, O.L., van der Heijden, G., Lewis, S.L., López-González, G., Aragão, L.E.O.C., Lloyd, J.
1445 et al.: Drought-mortality relationships for tropical forests, *New Phytol.*, 187, 631-646, 2010.

1446 Pilon, C.E., Côté, B., and Fyles, J.W.: Effect of an artificially induced drought on leaf peroxidase
1447 activity, mineral nutrition and growth of sugar maple, *Plant and Soil*, 179, 151-158, 1996.

1448 Potter, C., Klooster, S., Hiatt, C., Genovesi, V., and Castilla-Rubio, J.C.: Changes in the carbon
1449 cycle of Amazon ecosystems during the 2010 drought, *Environ. Res. Lett.*, 6, 034024, 2011.

1450 Powell, T.L., Galbraith, D.R., Christoffersen, B.O., Harper, A., Imbuzeiro, H.M.A., Rowland, L.
1451 et al.: Confronting model predictions of carbon fluxes with measurements of Amazon
1452 forests subjected to experimental drought, *New Phytol.*, 200, 350-365, 2013.

1453 Powell, T.L., Koven, C.D., Johnson, D.J., Faybishenko, B., Fisher, R.A., Knox, Ryan G. et al.:
1454 Variation in hydroclimate sustains tropical forest biomass and promotes functional diversity,
1455 *New Phytol.*, 219, 932-946, 2018.

1456 Powers, J.S., Becknell, J.M., Irving, J., and Pérez-Aviles, D.: Diversity and structure of
1457 regenerating tropical dry forests in Costa Rica: Geographic patterns and environmental
1458 drivers, *Forest Ecol. Manag.*, 258, 959-970, 2009.

1459 Powers, J.S., and Pérez-Aviles, D.: Edaphic Factors are a More Important Control on Surface
1460 Fine Roots than Stand Age in Secondary Tropical Dry Forests, *Biotropica*, 45, 1-9, 2013.

1461 Powers, JS, Vargas G., G, Brodribb, TJ, et al.: A catastrophic tropical drought kills hydraulically
1462 vulnerable tree species, *Glob. Change Biol.* 2020; 26: 3122– 3133,
1463 <https://doi.org/10.1111/gcb.15037>, 2020.

1464 Pugh, T.A.M., Rademacher, T., Shafer, S. L., Steinkamp, J., Barichivich, J., Beckage, B. et al.:
1465 Understanding the uncertainty in global forest carbon turnover, *Biogeosciences*, 17, 3961–
1466 3989, <https://doi.org/10.5194/bg-17-3961-2020>, 2020.

1467 Rapparini, F., and Peñuelas, J.: Mycorrhizal Fungi to Alleviate Drought Stress on Plant Growth.
1468 In: *Use of Microbes for the Alleviation of Soil Stresses*, Volume 1 (ed. Miransari, M),
1469 Springer New York New York, NY, pp. 21-42, 2014.

1470 Reich, P.B., Hobbie, S.E., and Lee, T.D.: Plant growth enhancement by elevated CO₂ eliminated
1471 by joint water and nitrogen limitation, *Nature Geoscience*, 7, 920, 2014.

1472 Reich, P.B., Wright, I.J., and Lusk, C.H.: PREDICTING LEAF PHYSIOLOGY FROM SIMPLE
1473 PLANT AND CLIMATE ATTRIBUTES: A GLOBAL GLOPNET ANALYSIS, *Ecological*
1474 *Applications*, 17, 1982-1988, 2007.

1475 Reichstein, M., Bahn, M., Ciais, P., Frank, D., Mahecha, M.D., Seneviratne, S.I. et al.: Climate
1476 extremes and the carbon cycle, *Nature*, 500, 287-295, 2013.

1477 Reyes, J.J., Tague, C.L., Evans, R.D., and Adam, J.C.: Assessing the Impact of Parameter
1478 Uncertainty on Modeling Grass Biomass Using a Hybrid Carbon Allocation Strategy, 9,
1479 2968-2992, 2017.

1480 Richardson, A.D., Carbone, M.S., Keenan, T.F., Czimczik, C.I., Hollinger, D.Y., Murakami, P. et
1481 al.: Seasonal dynamics and age of stemwood nonstructural carbohydrates in temperate forest
1482 trees, *New Phytol.*, 197, 850-861, 2013.

1483 Rowland, L., da Costa, A.C.L., Galbraith, D.R., Oliveira, R.S., Binks, O.J., Oliveira, A.A.R. et
1484 al.: Death from drought in tropical forests is triggered by hydraulics not carbon starvation,
1485 *Nature*, 528, 119, 2015.

1486 Roy, J., Picon-Cochard, C., Augusti, A., Benot, M.-L., Thiery, L., Darsonville, O. et al.: Elevated
1487 CO₂ maintains grassland net carbon uptake under a future heat and drought extreme, *PNAS*,
1488 113, 6224-6229, 2016.

1489 Ruppert, J.C., Harmony, K., Henkin, Z., Snyman, H.A., Sternberg, M., Willms, W. et al.:
1490 Quantifying drylands' drought resistance and recovery: the importance of drought intensity,
1491 dominant life history and grazing regime, *Glob. Change Biol.*, 21, 1258-1270, 2015.

1492 Rustad, L.E.: The response of terrestrial ecosystems to global climate change: Towards an
1493 integrated approach, *Science of The Total Environ.*, 404, 222-235, 2008.

1494 Ruthrof, K.X., Breshears, D.D., Fontaine, J.B., Froend, R.H., Matusick, G., Kala, J. et al.:
1495 Subcontinental heat wave triggers terrestrial and marine, multi-taxa responses, *Scientific*
1496 *Reports*, 8, 13094, 2018.

1497 Scheiter, S., Langan, L., and Higgins, S.I.: Next-generation dynamic global vegetation models:
1498 learning from community ecology, *New Phytol.*, 198, 957-969, 2013.

1499 Schenk, H.J., and Jackson, R.B.: Mapping the global distribution of deep roots in relation to
1500 climate and soil characteristics, *Geoderma*, 126, 129-140, 2005.

1501 Schwalm, C.R., Anderegg, W.R.L., Michalak, A.M., Fisher, J.B., Biondi, F., Koch, G. et al.:
1502 Global patterns of drought recovery, *Nature*, 548, 202, 2017.

1503 Seneviratne, S.I., X. Zhang, M. Adnan, W. Badi, C. Dereczynski, A. Di Luca, S. Ghosh, I.
1504 Iskandar, J. Kossin, S. Lewis, F. Otto, I. Pinto, M. Satoh, S.M. Vicente-Serrano, M. Wehner,
1505 and B. Zhou, 2021: Weather and Climate Extreme Events in a Changing Climate. In
1506 *Climate Change 2021: The Physical Science Basis. Contribution of Working Group I to the*
1507 *Sixth Assessment Report of the Intergovernmental Panel on Climate Change [Masson-*
1508 *Delmotte, V., P. Zhai, A. Pirani, S.L. Connors, C. Péan, S. Berger, N. Caud, Y. Chen, L.*
1509 *Goldfarb, M.I. Gomis, M. Huang, K. Leitzell, E. Lonnoy, J.B.R. Matthews, T.K. Maycock,*
1510 *T. Waterfield, O. Yelekçi, R. Yu, and B. Zhou (eds.)*, Cambridge University Press,
1511 Cambridge, United Kingdom and New York, NY, USA, pp. 1513–1766,
1512 doi:10.1017/9781009157896.013, 2021.

1513 Settele, J., Scholes, R., Betts, R., Bunn, S.E., Leadley, P., Nepstad, D., Overpeck, J.T., and
1514 Taboada, M.A.: Terrestrial and inland water systems. In: *Climate Change 2014: Impacts,*
1515 *Adaptation, and Vulnerability. Part A: Global and Sectoral Aspects. Contribution of*
1516 *Working Group II to the Fifth Assessment Report of the Intergovernmental Panel on*
1517 *Climate Change*, Cambridge University Press Cambridge, United Kingdom and New York,
1518 NY, USA, pp. 271-359, 2014.

1519 Sheffield, J., Goteti, G., and Wood, E.F.: Development of a 50-Year High-Resolution Global
1520 Dataset of Meteorological Forcings for Land Surface Modeling, *J. Climate*, 19, 3088-3111,
1521 2006.

1522 Shiels, A.B., Zimmerman, J.K., García-Montiel, D.C., Jonckheere, I., Holm, J., Horton, D. et al.:
1523 Plant responses to simulated hurricane impacts in a subtropical wet forest, Puerto Rico, *J.*
1524 *Ecology*, 98, 659-673, 2010.

1525 Silva, M., Matheny, A. M., Pauwels, V. R. N., Triadis, D., Missik, J. E., Bohrer, G., and Daly, E.:
1526 Tree hydrodynamic modelling of the soil–plant–atmosphere continuum using FETCH3,
1527 *Geosci. Model Dev.*, 15, 2619–2634, <https://doi.org/10.5194/gmd-15-2619-2022>, 2022.

1528 Sippel, S., Zscheischler, J., and Reichstein, M.: Ecosystem impacts of climate extremes crucially
1529 depend on the timing, *PNAS*, 113, 5768-5770, 2016.

1530 Sitch, S., HUNTINGFORD, C., GEDNEY, N., LEVY, P.E., LOMAS, M., PIAO, S.L. et al.:
1531 Evaluation of the terrestrial carbon cycle, future plant geography and climate-carbon cycle
1532 feedbacks using five Dynamic Global Vegetation Models (DGVMs), *Glob. Change Biol.*,
1533 14, 2015-2039, 2008.

1534 Skelton, R.P., West, A.G., and Dawson, T.E.: Predicting plant vulnerability to drought in
1535 biodiverse regions using functional traits, *PNAS*, 112, 5744-5749, 2015.

1536 Smith, B., Prentice, I.C., and Sykes, M.T.: Representation of vegetation dynamics in the
1537 modelling of terrestrial ecosystems: comparing two contrasting approaches within European
1538 climate space, *Global Ecol. Biogeo.*, 10, 621-637, 2001.

1539 Smith, B., Wärlind, D., Arneth, A., Hickler, T., Leadley, P., Siltberg, J. et al.: Implications of
1540 incorporating N cycling and N limitations on primary production in an individual-based
1541 dynamic vegetation model, *Biogeosciences*, 11, 2027-2054, 2014.

1542 Spasojevic, M.J., Bahlai, C.A., Bradley, B.A., Butterfield, B.J., Tuanmu, M.-N., Sistla, S. et al.:
1543 Scaling up the diversity–resilience relationship with trait databases and remote sensing data:
1544 the recovery of productivity after wildfire, *Glob. Change Biol.*, 22, 1421-1432, 2016.

1545 Sperry, J.S., Hacke, U.G., Oren, R., and Comstock, J.P.: Water deficits and hydraulic limits to
1546 leaf water supply, *Plant, Cell & Environ.*, 25, 251-263, 2002.

1547 Sperry, J.S., and Love, D.M.: What plant hydraulics can tell us about responses to climate-change
1548 droughts, *New Phytol.*, 207, 14-27, 2015.

1549 Sperry, J.S., Wang, Y., Wolfe, B.T., Mackay, D.S., Anderegg, W.R.L., McDowell, N.G. et al.:
1550 Pragmatic hydraulic theory predicts stomatal responses to climatic water deficits, *New*
1551 *Phytol.*, 212, 577-589, 2016.

1552 Stovall, A.E.L., Shugart, H., and Yang, X.: Tree height explains mortality risk during an intense
1553 drought, *Nature Communications*, 10, 4385, 2019.

1554 Tague, C.L., and Moritz, M.A.: Plant Accessible Water Storage Capacity and Tree-Scale Root
1555 Interactions Determine How Forest Density Reductions Alter Forest Water Use and
1556 Productivity, *Front. Forests and Global Change*, 2, 2019.

1557 Tomasella M, Petrusa E, Petruzzellis F, Nardini A, Casolo V.: The Possible Role of Non-
1558 Structural Carbohydrates in the Regulation of Tree Hydraulics, *International Journal of*
1559 *Molecular Sciences*, 21:144, <https://doi.org/10.3390/ijms21010144>, 2020.

1560 Trugman, A.T., Detto, M., Bartlett, M.K., Medvigy, D., Anderegg, W.R.L., Schwalm, C. et al.:
1561 Tree carbon allocation explains forest drought-kill and recovery patterns, *Ecol. Lett.*, 21,
1562 1552-1560, 2018.

1563 Trugman, A.T., Anderegg, L.D.L., Sperry, J.S., Wang, Y., Venturas, M., Anderegg,
1564 W.R.L.: Leveraging plant hydraulics to yield predictive and dynamic plant leaf allocation in
1565 vegetation models with climate change, *Glob. Change*
1566 *Biol.*, 25, 4008– 4021. <https://doi.org/10.1111/gcb.14814>, 2019.

1567 Uriarte, M., Lasky, J.R., Boukili, V.K., and Chazdon, R.L.: A trait-mediated, neighbourhood
1568 approach to quantify climate impacts on successional dynamics of tropical rainforests,
1569 *Funct. Ecol.*, 30, 157-167, 2016.

1570 Vargas G., G., Brodribb, T.J., Dupuy, J.M., González-M., R., Hulshof, C.M., Medvigy, D.,
1571 Allerton, T.A.P., Pizano, C., Salgado-Negret, B., Schwartz, N.B., Van Bloem, S.J., Waring,
1572 B.G. and Powers, J.S.: Beyond leaf habit: generalities in plant function across 97 tropical
1573 dry forest tree species, *New Phytol.*, 232: 148-161. <https://doi.org/10.1111/nph.17584>, 2021.

1574 Venturas, M. D., Todd, H. N., Trugman, A. T., and Anderegg, W. R.: Understanding and
1575 predicting forest mortality in the western United States using long-term forest inventory data
1576 and modeled hydraulic damage, *New Phytol.*, 230, 1896-1910, 2021.

1577 Wang, D., Heckathorn, S.A., Wang, X., and Philpott, S.M.: A meta-analysis of plant
1578 physiological and growth responses to temperature and elevated CO₂, *Oecologia*, 169, 1-13,
1579 2012.

1580 Weng, E.S., Malyshev, S., Lichstein, J.W., Farrior, C.E., Dybzinski, R., Zhang, T. et al.: Scaling
1581 from individual trees to forests in an Earth system modeling framework using a
1582 mathematically tractable model of height-structured competition, *Biogeosciences*, 12, 2655-
1583 2694, 2015.

1584 Williams, A.P., Allen, C.D., Macalady, A.K., Griffin, D., Woodhouse, C.A., Meko, D.M. et al.:
1585 Temperature as a potent driver of regional forest drought stress and tree mortality, *Nature*
1586 *Climate Change*, 3, 292, 2012.

1587 Williams, A.P., Seager, R., Berkelhammer, M., Macalady, A.K., Crimmins, M.A., Swetnam,
1588 T.W. et al.: Causes and Implications of Extreme Atmospheric Moisture Demand during the
1589 Record-Breaking 2011 Wildfire Season in the Southwestern United States, *J. Applied*
1590 *Meteorology and Climatology*, 53, 2671-2684, 2014.

- 1591 Williams, L.J., Bunyavejchewin, S., and Baker, P.J.: Deciduousness in a seasonal tropical forest
1592 in western Thailand: interannual and intraspecific variation in timing, duration and
1593 environmental cues, *Oecologia*, 155, 571-582, 2008.
- 1594 Wullschleger, S.D., Hanson, P.J., and Todd, D.E.: Transpiration from a multi-species deciduous
1595 forest as estimated by xylem sap flow techniques, *For. Ecol. and Manage.*, 143, 205-213,
1596 2001.
- 1597 Xu, X., Medvigy, D., Powers, J.S., Becknell, J.M. and Guan, K.: Diversity in plant hydraulic
1598 traits explains seasonal and inter-annual variations of vegetation dynamics in seasonally dry
1599 tropical forests, *New Phytol.*, 212, 80-95, 2016.
- 1600 Yang, Y., Hillebrand, H., Lagisz, M., Cleasby, I., and Nakagawa, S.: Low statistical power and
1601 overestimated anthropogenic impacts, exacerbated by publication bias, dominate field
1602 studies in global change biology. *Glob. Change Biol.*, 28, 969– 989,
1603 <https://doi.org/10.1111/gcb.15972>, 2022.
- 1604 Zhu, K., Chiariello, N.R., Tobeck, T., Fukami, T., and Field, C.B.: Nonlinear, interacting
1605 responses to climate limit grassland production under global change, *PNAS*, 113, 10589-
1606 10594, 2016.
- 1607 Zhu, S-D., Chen, Y-J., Ye, Q., He, P-C., Liu, H., and Li, R-H., et al.: Leaf turgor loss point is
1608 correlated with drought tolerance and leaf carbon economics traits, *Tree Physiol.*, 38, 658–
1609 663, <https://doi.org/10.1093/treephys/tpy013>, 2018.
- 1610 Zscheischler, J., Mahecha, M.D., von Buttlar, J., Harmeling, S., Jung, M., Rammig, A. et al.: A
1611 few extreme events dominate global interannual variability in gross primary production,
1612 *Environ. Res. Lett.*, 9, 035001, 2014.